



**HAL**  
open science

# Adaptive inexact smoothing Newton method for a nonconforming discretization of a variational inequality

Ibtihel Ben Gharbia, Joëlle Ferzly, Martin Vohralík, Soleiman Yousef

## ► To cite this version:

Ibtihel Ben Gharbia, Joëlle Ferzly, Martin Vohralík, Soleiman Yousef. Adaptive inexact smoothing Newton method for a nonconforming discretization of a variational inequality. 2022. hal-03696024v1

**HAL Id: hal-03696024**

**<https://inria.hal.science/hal-03696024v1>**

Preprint submitted on 15 Jun 2022 (v1), last revised 22 Nov 2022 (v2)

**HAL** is a multi-disciplinary open access archive for the deposit and dissemination of scientific research documents, whether they are published or not. The documents may come from teaching and research institutions in France or abroad, or from public or private research centers.

L'archive ouverte pluridisciplinaire **HAL**, est destinée au dépôt et à la diffusion de documents scientifiques de niveau recherche, publiés ou non, émanant des établissements d'enseignement et de recherche français ou étrangers, des laboratoires publics ou privés.

# Adaptive inexact smoothing Newton method for a nonconforming discretization of a variational inequality\*

Ibtihel Ben Gharbia<sup>†</sup> Joëlle Ferzly<sup>†‡§</sup> Martin Vohralík<sup>‡§</sup> Soleiman Yousef<sup>†</sup>

June 7, 2022

## Abstract

We develop in this work an adaptive inexact smoothing Newton method for a nonconforming discretization of a variational inequality. As a model problem, we consider the contact problem between two membranes. Discretized with the finite volume method, this leads to a nonlinear algebraic system with complementarity constraints. The non-differentiability of the arising nonlinear discrete problem a priori requests the use of an iterative linearization algorithm in the semismooth class like, e.g., the Newton-min. In this work, we rather approximate the inequality constraints by a smooth nonlinear equality, involving a positive smoothing parameter that should be drawn down to zero. This makes it possible to directly apply any standard linearization like the Newton method. The solution of the ensuing linear system is then approximated by any iterative linear algebraic solver. In our approach, we carry out an a posteriori error analysis where we introduce potential reconstructions in discrete subspaces included in  $H^1(\Omega)$ , as well as  $\mathbf{H}(\text{div}, \Omega)$ -conforming discrete equilibrated flux reconstructions. With these elements, we design an a posteriori estimate that provides guaranteed upper bound on the energy error between the unavailable exact solution of the continuous level and a postprocessed, discrete, and available approximation, and this at any resolution step. It also offers a separation of the different error components, namely, discretization, smoothing, linearization, and algebraic. Moreover, we propose stopping criteria and design an adaptive algorithm where all the iterative procedures (smoothing, linearization, algebraic) are adaptively stopped; this is in particular our way to fix the smoothing parameter. Finally, we numerically assess the estimate and confirm the performance of the proposed adaptive algorithm, in particular in comparison with the semismooth Newton method.

**Key words:** elliptic variational inequality, complementarity constraint, semismooth and smoothing Newton method, equilibrated flux, a posteriori error estimate, stopping criteria

## 1 Introduction

Variational inequalities have been of great interest to researchers due to their various applications. Possibly expressed as a system of partial differential equations (PDEs) with complementarity constraints, they arise in a variety of fields such as engineering and economics [30], mathematical finance [31], structural mechanics [17], flow processes in porous media [10], and many more. The numerical discretization of such problems yields a finite-dimensional nonlinear algebraic system with complementarity constraints written in the form: find a vector  $\mathbf{X} \in \mathbb{R}^n$ ,  $n > 1$ , such that

$$\mathbb{E}\mathbf{X} = \mathbf{F}, \tag{1.1a}$$

$$\mathbf{K}(\mathbf{X}) \geq \mathbf{0}, \mathbf{G}(\mathbf{X}) \geq \mathbf{0}, \mathbf{K}(\mathbf{X}) \cdot \mathbf{G}(\mathbf{X}) = 0. \tag{1.1b}$$

Let  $0 < m < n$  be an integer. The first line (1.1a) derives from the discretization of a linear PDE, where  $\mathbb{E} \in \mathbb{R}^{n-m, n}$  is a matrix and  $\mathbf{F} \in \mathbb{R}^{n-m}$  is a given vector. Denoting by  $\mathbf{K} : \mathbb{R}^n \rightarrow \mathbb{R}^m$  and  $\mathbf{G} : \mathbb{R}^n \rightarrow \mathbb{R}^m$  two (linear) operators, line (1.1b) expresses the complementarity relationship between the nonnegative vectors  $\mathbf{K}(\mathbf{X})$  and  $\mathbf{G}(\mathbf{X})$ , in the sense that if one of them has a positive component, then the corresponding component in the other one must be zero. Countless developments have been made over the years to (approximately) solve problem (1.1). In this regard, we mention the semismooth Newton method [18, 36, 9], the active set-type

\*This project has partly received funding from the European Research Council (ERC) under the European Union's Horizon 2020 research and innovation program (grant agreement No 647134 GATIPOR).

<sup>†</sup>IFP Energies nouvelles, 1 et 4 avenue de Bois-Préau, 92852 Rueil-Malmaison, France ([ibtihel.ben-gharbia@ifpen.fr](mailto:ibtihel.ben-gharbia@ifpen.fr), [joelle.ferzly@ifpen.fr](mailto:joelle.ferzly@ifpen.fr), [soleiman.yousef@ifpen.fr](mailto:soleiman.yousef@ifpen.fr)).

<sup>‡</sup>Inria, 2 Rue Simone Lff, 75589 Paris, France ([martin.vohralik@inria.fr](mailto:martin.vohralik@inria.fr)).

<sup>§</sup>CERMICS, Ecole des Ponts, 77455 Marne-la-Vallée, France

14 methods [42], the primal-dual active set strategy which can be interpreted as a semismooth Newton method  
 15 [38], and projection-type methods [59]. Another class of methods, motivated by the augmented Lagrangian  
 16 methods, is the one invoking a regularization technique [51, 41]. It can be combined with a path-following  
 17 strategy to properly update the regularization parameter, see, e.g., [39, 52]. Inspired from the interior-point  
 18 methods [58, 35], another approach is the non-parametric interior-point method proposed recently in [57]. For  
 19 an enlightening summary of numerical methods solving problem (1.1), we refer to the books of Ferris et al. [29],  
 20 Facchinei and Pang [27, 28], Bonnans et al. [11], Ito and Kunisch [40], and Ulbrich [53].

21 In this work, we focus on smoothing Newton methods. The guiding principle of this approach is to ap-  
 22 proximate the complementarity constraints in (1.1b) by a system of smooth (differentiable) nonlinear equations  
 23  $\mathbf{C}_\mu(\mathbf{X}) = \mathbf{0}$ , where  $\mathbf{C}_\mu : \mathbb{R}^n \rightarrow \mathbb{R}^m$  is a smooth (differentiable) approximation of a non-differentiable com-  
 24 plementarity function (C-function)  $\mathbf{C} : \mathbb{R}^n \rightarrow \mathbb{R}^m$  with a parameter  $\mu > 0$ . This reformulation brings us to  
 25 approximate problem (1.1) at each smoothing step  $j \geq 1$ , with parameter  $\mu^j > 0$ , by finding a vector  $\mathbf{X}^j \in \mathbb{R}^n$   
 26 such that

$$\begin{aligned} \mathbb{E}\mathbf{X}^j &= \mathbf{F}, \\ \mathbf{C}_{\mu^j}(\mathbf{X}^j) &= \mathbf{0}. \end{aligned} \quad (1.2)$$

27 Hence, any iterative linearization procedure can be directly applied to system (1.2), yielding at each linearization  
 28 step  $k \geq 1$  a linear system

$$\mathbb{A}_{\mu^j}^{j,k-1} \mathbf{X}^{j,k} = \mathbf{B}_{\mu^j}^{j,k-1}, \quad (1.3)$$

29 where  $\mathbb{A}_{\mu^j}^{j,k-1} \in \mathbb{R}^{n,n}$  is a matrix and  $\mathbf{B}_{\mu^j}^{j,k-1} \in \mathbb{R}^n$  is a vector. Let us stress, however, that it is impractical to  
 30 solve (1.3) exactly in applications. Following [26, 43, 49, 32], we solve the latter system only approximately  
 31 by employing an iterative linear algebraic solver, giving rise, at each smoothing step  $j \geq 1$ , linearization step  
 32  $k \geq 1$ , and linear algebraic step  $i \geq 1$ , to a residual vector  $\mathbf{R}_{\text{alg}}^{j,k,i} \in \mathbb{R}^n$  defined by

$$\mathbf{R}_{\text{alg}}^{j,k,i} := \mathbf{B}_{\mu^j}^{j,k-1} - \mathbb{A}_{\mu^j}^{j,k-1} \mathbf{X}^{j,k,i}. \quad (1.4)$$

33 In this regard, as we consider numerical approximations, it is crucial to control the error between the unknown  
 34 PDE solution  $\mathbf{u}$  and the numerical approximation arising at steps  $j, k, i$ , say  $\mathbf{u}_h^{j,k,i}$ , and to approximate systems  
 35 (1.2), (1.3), and (1.4) efficiently and accurately while limiting the computational costs. The present paper  
 36 aims at designing an adaptive algorithm steering the iterations in  $j, k$ , and  $i$ . Our key tool for this is to derive  
 37 guaranteed a posteriori estimates allowing to obtain a fully computable upper bound on the energy error  $e^{j,k,i}$   
 38 between the approximate solution  $\mathbf{u}_h^{j,k,i}$  and the unknown solution  $\mathbf{u}$ , at each step  $j \geq 1, k \geq 1$ , and  $i \geq 1$  of  
 39 the resolution, in the form

$$e^{j,k,i} \leq \eta_{\text{disc}}^{j,k,i} + \eta_{\text{sm}}^{j,k,i} + \eta_{\text{lin}}^{j,k,i} + \eta_{\text{alg}}^{j,k,i}. \quad (1.5)$$

40 These computable estimates allow us to identify all sources of error resulting from the numerical simulation,  
 41 namely the discretization, smoothing, linearization, and linear algebraic solver error. Distinguishing the error  
 42 components in particular enables to formulate optimal criteria to adaptively stop the various iterative solvers  
 43 whenever the corresponding error no longer significantly influences the behavior of the overall error, as in  
 44 [45, 4, 22, 20, 48, 16, 17, 37, 34], and the references therein.

45 There is a well-developed literature on a posteriori error estimates for PDEs. For a general introduction,  
 46 we refer for instance to the books of Ainsworth and Oden [2], Repin [46], and Verfürth [54]. For variational  
 47 inequalities, we can mention the contributions of Repin [47], Belgacem et al. [7], and Bürg and Schröder [15].  
 48 In this work, we are interested in the so-called equilibrated fluxes estimates, based on  $\mathbf{H}(\text{div}, \Omega)$ -conforming  
 49 and locally conservative flux reconstructions belonging to the lowest-order Raviart–Thomas–Nédélec space  $\mathbf{RT}_0$   
 50 (discrete subspace of  $\mathbf{H}(\text{div}, \Omega)$ ). We refer the reader to the contributions [19, 12, 22]. As we consider a  
 51 nonconforming, finite volume, numerical discretization, we will also rely on a potential reconstruction following  
 52 in particular [1, 56, 23]. This methodology in particular allows us to obtain the unknown constant-free bound  
 53 in (1.5).

54 We apply our approach to the following problem that models the contact between two membranes. Let  
 55  $\Omega \subset \mathbb{R}^2$  be an open polygonal domain. The problem reads: find  $u_1, u_2$ , and  $\lambda$  such that

$$\begin{cases} -\beta_1 \Delta u_1 - \lambda = f_1 & \text{in } \Omega, & (1.6a) \\ -\beta_2 \Delta u_2 + \lambda = f_2 & \text{in } \Omega, & (1.6b) \\ u_1 - u_2 \geq 0, \quad \lambda \geq 0, \quad (u_1 - u_2)\lambda = 0 & \text{in } \Omega, & (1.6c) \\ u_1 = g & \text{on } \partial\Omega, & (1.6d) \\ u_2 = 0 & \text{on } \partial\Omega, & (1.6e) \end{cases}$$

56 where the unknowns are the displacements  $u_1$  and  $u_2$  of the two membranes and the Lagrange multiplier  $\lambda$   
57 which characterizes the action, or the reaction  $-\lambda$ , of one membrane on the other. Equations (1.6a) and (1.6b)  
58 describe the kinematic behavior of each membrane under the action of external forces  $f_1, f_2 \in L^2(\Omega)$ . The  
59 constant parameters  $\beta_1, \beta_2 > 0$  correspond to the tension of each membrane. Line (1.6c) represents the linear  
60 complementarity conditions,  $u_1 - u_2 \geq 0$  states that the membranes cannot interpenetrate,  $\lambda \geq 0$  stems from  
61 the definition of  $\lambda$ , and  $(u_1 - u_2)\lambda = 0$  means that where the membranes are not in contact ( $u_1 - u_2 > 0$ ),  $\lambda$   
62 vanishes, and where they are in contact ( $u_1 = u_2$ ),  $\lambda$  is nonnegative. The boundary conditions in (1.6d) and  
63 (1.6e) indicate that the first membrane is fixed on the boundary  $\partial\Omega$  at  $g > 0$ , where  $g$  is a constant, above the  
64 second one, which is fixed at zero.

65 The contact problem (1.6) has been studied in several works. Existence and uniqueness together with a  
66 conforming finite element discretization were studied in [5, 6, 7], see also the references therein. A semismooth  
67 Newton method combined with a path-following strategy was introduced and tested in [60]. Recently, in [17],  
68 an adaptive inexact Newton method, steered by a posteriori error estimates as in (1.5), was proposed to solve  
69 problem (1.6) when discretized by conforming finite elements. In our work, we rather consider the cell-centered  
70 finite volume method. We develop an adaptive inexact smoothing Newton method to solve the arising discrete  
71 problem, where any of the classical linearization scheme for smooth nonlinearities and any iterative linear  
72 algebraic solver can be used.

73 Let us briefly outline the structure of the paper. In Section 2, we fix notation, present the model problem  
74 (1.6) in details, and introduce its finite volume discretization. We recall the semismooth Newton method in  
75 Section 3. Then, we introduce a smoothed reformulation of our problem and address its numerical approximation  
76 employing an (inexact) smoothing Newton method in Section 4. Next, Sections 5 and 6 are devoted to describe  
77 the potential and equilibrated flux reconstructions, enabling to pursue our analysis. In Section 7, we derive  
78 an a posteriori error estimate on the error between the exact solution and the approximate solution on any  
79 smoothing step  $j \geq 1$ , any linearization step  $k \geq 1$ , and any algebraic step  $i \geq 1$ . We split our guaranteed bound  
80 into estimators characterizing the discretization, smoothing, and algebraic errors, and establish a linearization  
81 estimator reflecting the linearization error, obtaining an estimate of the form (1.5). This error distinction leads  
82 to adaptive stopping criteria that we incorporate in the adaptive inexact smoothing Newton algorithm presented  
83 in Section 8. We study numerically the behavior of our a posteriori estimates and the efficiency of the developed  
84 algorithm in Section 9. Finally, Section 10 brings forth our conclusions and outlook.

## 85 2 Continuous problem and its finite volume discretization

86 In this section, we first fix notation and present the full and reduced variational formulations of the model  
87 problem (1.6). Then, we introduce its finite volume discretization.

### 88 2.1 Function spaces, meshes, and notation

89 We first recall the definition of some functional spaces. For a domain  $\Omega \subset \mathbb{R}^2$ , let  $\mathcal{D}(\Omega)$  be the space of functions  
90  $u : \Omega \rightarrow \mathbb{R}$  of class  $C^\infty$  with a compact support in  $\Omega$ . We denote by  $L^2(\Omega)$  the space of Lebesgue-measurable  
91 functions  $u : \Omega \rightarrow \mathbb{R}$  such that  $\|u\| := (\int_\Omega |u(x)|^2 dx)^{\frac{1}{2}} < \infty$ . It is a Hilbert space for the scalar product  
92  $(u, v) = \int_\Omega u(x)v(x)dx$ . Next,  $H^1(\Omega)$  stands for the space of functions in  $L^2(\Omega)$  which admit a weak gradient in  
93  $[L^2(\Omega)]^2$ , and  $H_0^1(\Omega)$  stands for its subspace of functions that vanish on  $\partial\Omega$  in the sense of traces. Moreover,  
94  $\mathbf{H}(\text{div}, \Omega)$  is the space of vector-valued functions  $\mathbf{u} : \Omega \rightarrow \mathbb{R}^2$ ,  $\mathbf{u} \in [L^2(\Omega)]^2$ , such that  $\nabla \cdot \mathbf{u} \in L^2(\Omega)$ . The  
95 standard notation  $\nabla \cdot$  is used for the weak divergence operator. We shall define the sets

$$H_g^1(\Omega) := \{u \in H^1(\Omega), u = g \text{ on } \partial\Omega\} \text{ and } \Lambda := \{\chi \in L^2(\Omega), \chi \geq 0 \text{ a.e. in } \Omega\}.$$

96 We also use in the subsequent sections the notation  $\|\cdot\|_\omega := (\cdot, \cdot)_\omega$  for the  $L^2(\omega)$  norm and scalar product on a  
97 subdomain  $\omega$  of  $\Omega$ . When  $\omega = \Omega$ , the subscript is dropped. A similar notation is used for vector-valued functions.  
98

99 We shall consider a mesh  $\mathcal{T}_h$  given by a family of triangles  $K$  verifying  $\bar{\Omega} = \bigcup_{K \in \mathcal{T}_h} \bar{K}$ . We assume that  
100 the elements of  $\mathcal{T}_h$  are conforming in the sense that the intersection of the closure of two elements is either an  
101 empty set, a vertex, or an edge. We also assume that  $\mathcal{T}_h$  is admissible, i.e., for all  $K \in \mathcal{T}_h$ , there is an associated  
102 point  $x_K$  such that the straight line connecting two points  $x_K$  and  $x_L$  of two neighboring triangles  $K$  and  
103  $L \in \mathcal{T}_h$  is orthogonal to  $\sigma_{K,L} := \partial K \cap \partial L$ , see [24]; we choose for  $x_K$  the circumcenter of  $K$ . We denote by  $\mathcal{E}_h$   
104 the set of all edges  $\sigma$  of  $\mathcal{T}_h$ , by  $\mathcal{E}_h^{\text{int}}$  the set of interior, and by  $\mathcal{E}_h^{\text{ext}}$  the set of boundary edges. To each edge  
105  $\sigma \in \mathcal{E}_h$ , we associate a unit normal vector  $\mathbf{n}_\sigma$ . The set of all edges of  $K$  is denoted by  $\mathcal{E}_K$ , which is decomposed  
106 into interior edges and boundary edges such that  $\mathcal{E}_K = \mathcal{E}_K^{\text{int}} \cup \mathcal{E}_K^{\text{ext}}$ . We denote by  $\mathbf{n}_{K,\sigma}$  the outward unit normal

107 vector to  $K$  on the edge  $\sigma$ .

108

109 We then define the broken Sobolev space  $H^1(\mathcal{T}_h) := \{u \in L^2(\Omega); u|_K \in H^1(K), \forall K \in \mathcal{T}_h\}$ . For a func-  
 110 tion  $u \in H^1(\mathcal{T}_h)$ , we denote by  $\nabla u \in [L^2(\Omega)]^2$  the broken weak gradient such that  $(\nabla u)|_K := \nabla(u|_K)$ .

111

112 Next, for a function  $u$  and an edge  $\sigma \in \mathcal{E}_h^{\text{int}}$  shared by  $K, L \in \mathcal{T}_h$  such that  $\mathbf{n}_\sigma$  points from  $K$  towards  $L$ , we  
 113 define the jump of  $u$  on  $\sigma$  as

$$\llbracket u \rrbracket_\sigma := (u|_K)|_\sigma - (u|_L)|_\sigma.$$

114 We set  $\llbracket u \rrbracket_\sigma = u|_\sigma$  for  $\sigma \in \mathcal{E}_h^{\text{ext}}$  in the contact of the second membrane, whereas  $\llbracket u \rrbracket_\sigma = u|_\sigma - g$  for the first  
 115 membrane and its approximations. Later, we will simply use the notation  $\llbracket u \rrbracket$ , since there will be no ambiguity,  
 116 and also extend it componentwise for vector-valued variables.

117 We recall two basic inequalities that will be necessary in order to carry out the analysis in the following  
 118 sections. Let  $h_\omega$  denote the diameter of  $\omega \subset \Omega$ . The Poincaré–Friedrichs and the Poincaré–Wirtinger inequalities  
 119 state that

$$\|u\|_\omega \leq C_{\text{PF}} h_\omega \|\nabla u\|_\omega \quad \forall u \in H_0^1(\omega), \quad (2.1a)$$

$$\|u - \bar{u}_\omega\|_\omega \leq C_{\text{PW}} h_\omega \|\nabla u\|_\omega \quad \forall u \in H^1(\omega), \quad (2.1b)$$

120 where  $\bar{u}_\omega$  is the mean value of the function  $u$  over  $\omega$  given by  $\bar{u}_\omega := (u, 1)_\omega / |\omega|$  ( $|\omega|$  is the measure of  $\omega$ ).  
 121 The constant  $C_{\text{PF}}$  can be taken equal to 1, cf. [55, Remark 5.8]. If  $\omega$  is convex,  $C_{\text{PW}}$  can be evaluated  
 122 as  $1/\pi$ , cf. [3], and it only depends on the geometry of  $\omega$  if  $\omega$  is non-convex, cf. [24, Lemma 10.4]. For a  
 123 function  $\mathbf{u} = (u_1, u_2) \in [H_0^1(\omega)]^2$ , we introduce the energy semi-norm

$$\|\mathbf{u}\|_\omega := \left\{ \sum_{\alpha=1}^2 \beta_\alpha \|\nabla u_\alpha\|_\omega^2 \right\}^{\frac{1}{2}}. \quad (2.2)$$

124 We will use the simplified notation  $\|\mathbf{u}\| := \|\mathbf{u}\|_\omega$  when  $\omega = \Omega$ . We extend this definition in the same way  
 125 to all  $\mathbf{u} = (u_1, u_2) \in [H^1(\mathcal{T}_h)]^2$ , where it becomes merely a semi-norm. Finally, we define the rescaling of the  
 126  $H^{-1}(\omega)$  norm

$$\|\mathbf{u}\|_{H_*^{-1}(\omega)} := \sup_{\substack{\phi \in H_0^1(\omega) \\ \max(\beta_1^{\frac{1}{2}}, \beta_2^{\frac{1}{2}}) \|\nabla \phi\|_\omega = 1}} \langle \mathbf{u}, \phi \rangle, \quad \mathbf{u} \in H^{-1}(\omega). \quad (2.3)$$

## 127 2.2 Continuous problem

128 Setting  $\mathbf{u} := (u_1, u_2)$  and  $\mathbf{v} := (v_1, v_2) \in [H^1(\Omega)]^2$ , we consider the forms, for  $\chi \in L^2(\Omega)$ ,

$$a(\mathbf{u}, \mathbf{v}) := \sum_{\alpha=1}^2 \beta_\alpha (\nabla u_\alpha, \nabla v_\alpha), \quad b(\mathbf{v}, \chi) := (\chi, v_1 - v_2), \quad l(\mathbf{v}) := \sum_{\alpha=1}^2 (f_\alpha, v_\alpha). \quad (2.4)$$

129 We will also consider in a forthcoming section the extension

$$a(\mathbf{u}, \mathbf{v}) := \sum_{\alpha=1}^2 \beta_\alpha (\nabla u_\alpha, \nabla v_\alpha) \quad \mathbf{u}, \mathbf{v} \in [H^1(\mathcal{T}_h)]^2, \quad (2.5)$$

130 where, recall,  $\nabla$  denotes the broken weak gradient on  $H^1(\mathcal{T}_h)$ .

131

132 Given  $(f_1, f_2) \in [L^2(\Omega)]^2$  and  $g > 0$  a constant, the weak formulation of problem (1.6) is to find  $\mathbf{u} \in$   
 133  $H_g^1(\Omega) \times H_0^1(\Omega)$  and  $\lambda \in \Lambda$  such that

$$a(\mathbf{u}, \mathbf{v}) - b(\mathbf{v}, \lambda) = l(\mathbf{v}) \quad \forall \mathbf{v} \in [H_0^1(\Omega)]^2, \quad (2.6a)$$

$$b(\mathbf{u}, \chi - \lambda) \geq 0 \quad \forall \chi \in \Lambda. \quad (2.6b)$$

134 Problem (2.6) admits a unique weak solution (cf. [6, Proposition 1]).

135 Define then the convex set  $\mathcal{K}_g$  by

$$\mathcal{K}_g := \{(v_1, v_2) \in H_g^1(\Omega) \times H_0^1(\Omega), v_1 - v_2 \geq 0 \text{ a.e. in } \Omega\}. \quad (2.7)$$

136 We also consider the reduced variational problem: find  $\mathbf{u} = (u_1, u_2) \in \mathcal{K}_g$  such that

$$a(\mathbf{u}, \mathbf{v} - \mathbf{u}) \geq l(\mathbf{v} - \mathbf{u}) \quad \forall \mathbf{v} = (v_1, v_2) \in \mathcal{K}_g, \quad (2.8)$$

137 which is equivalent to (2.6), as proved in [6, Lemma 2]. Note that by the Poincaré–Friedrichs inequality  
 138 (2.1a), the bilinear form  $a$  is coercive on  $[H_0^1(\Omega)]^2$ . Thus, the well-posedness of (2.8) is a consequence of the  
 139 Lions–Stampacchia theorem, see [13, Theorem 5.6].

## 140 2.3 Finite volume discretization

141 The finite volume scheme for problem (1.6) reads: find the values  $\{u_{1,K}\}_{K \in \mathcal{T}_h}$ ,  $\{u_{2,K}\}_{K \in \mathcal{T}_h}$ , and  $\{\lambda_K\}_{K \in \mathcal{T}_h}$   
 142 such that for all  $K \in \mathcal{T}_h$

$$\sum_{\sigma \in \mathcal{E}_K} F_{\alpha,K,\sigma} + (-1)^\alpha |K| \lambda_K = |K| f_{\alpha,K}, \quad \alpha \in \{1, 2\}, \quad (2.9a)$$

$$u_{1,K} - u_{2,K} \geq 0, \quad \lambda_K \geq 0, \quad (u_{1,K} - u_{2,K}) \lambda_K = 0, \quad (2.9b)$$

143 where  $f_{\alpha,K} := (f_\alpha, 1)/|K|$ . In scheme (2.9),  $F_{\alpha,K,\sigma}$  represents the numerical approximation of the flux through  
 144 the edge  $\sigma$  of the element  $K \in \mathcal{T}_h$  and is given by

$$F_{\alpha,K,\sigma} = \begin{cases} -\beta_\alpha |\sigma| \frac{u_{\alpha,L} - u_{\alpha,K}}{d_{K,L}} & \text{if } \sigma \in \mathcal{E}_h^{\text{int}}, \sigma = K \cap L, \\ -\beta_\alpha |\sigma| \frac{u_{\alpha,\sigma} - u_{\alpha,K}}{d_{K,\sigma}} & \text{if } \sigma \in \mathcal{E}_h^{\text{ext}}, \end{cases} \quad (2.10)$$

145 where for  $\sigma \in \mathcal{E}_h^{\text{ext}}$ ,  $u_{1,\sigma} = g$  and  $u_{2,\sigma} = 0$ , which corresponds to the discretization of the Dirichlet boundary  
 146 conditions in (1.6). Let for the discretization of problem (1.6),  $m$  denotes the number of mesh elements and  $n :=$   
 147  $3m$ . Using that  $\mathcal{E}_K = \mathcal{E}_K^{\text{int}} \cup \mathcal{E}_K^{\text{ext}}$ , we develop (2.9) and define the stiffness matrix  $\mathbb{C}_\alpha \in \mathbb{R}^{m,m}$ ,  $\alpha \in \{1, 2\}$ , by

$$\mathbb{C}_{\alpha,K,K} := \sum_{\sigma \in \mathcal{E}_K^{\text{int}}} \frac{|\sigma|}{d_{K,L}} + \sum_{\sigma \in \mathcal{E}_K^{\text{ext}}} \frac{|\sigma|}{d_{K,\sigma}}, \quad \mathbb{C}_{\alpha,K,L} := -\frac{|\sigma|}{d_{K,L}}, \quad K, L \in \mathcal{T}_h, K \neq L.$$

148 We also define the diagonal mass matrix  $\mathbb{M} \in \mathbb{R}^{m,m}$  by  $\mathbb{M}_{K,K} := |K|$ , and a vector  $\mathbf{f}_\alpha \in \mathbb{R}^m$  such that  
 149  $\mathbf{f}_{\alpha,K} := |K| f_{\alpha,K} + \sum_{\sigma \in \mathcal{E}_K^{\text{ext}}} \beta_\alpha \frac{|\sigma|}{d_{K,\sigma}} u_{\alpha,\sigma}$ ,  $\forall K \in \mathcal{T}_h$ . Let  $\mathbf{X} := [\mathbf{X}_1, \mathbf{X}_2, \boldsymbol{\lambda}]^T \in \mathbb{R}^n$  be the algebraic vector of  
 150 unknowns of the model such that  $\mathbf{X}_1 = (u_{1,K})_{K \in \mathcal{T}_h} \in \mathbb{R}^m$ ,  $\mathbf{X}_2 = (u_{2,K})_{K \in \mathcal{T}_h} \in \mathbb{R}^m$ , and  $\boldsymbol{\lambda} = (\lambda_K)_{K \in \mathcal{T}_h} \in \mathbb{R}^m$ .  
 151 Then, the finite volume discretization (2.9a) can be written as: find  $\mathbf{X} \in \mathbb{R}^n$  such that  $\mathbb{E}\mathbf{X} = \mathbf{F}$ , with  
 152  $\mathbf{F} := [\mathbf{f}_1, \mathbf{f}_2]^T \in \mathbb{R}^{n-m}$  being the right-hand side vector, and  $\mathbb{E} \in \mathbb{R}^{n-m,n}$  being a rectangular block matrix  
 153 defined by

$$\mathbb{E} := \begin{bmatrix} \beta_1 \mathbb{C}_1 & \mathbf{0} & -\mathbb{M} \\ \mathbf{0} & \beta_2 \mathbb{C}_2 & \mathbb{M} \end{bmatrix}.$$

154 Overall, (2.9) leads to the following system of algebraic inequalities: find  $\mathbf{X} \in \mathbb{R}^n$  such that

$$\mathbb{E}\mathbf{X} = \mathbf{F}, \quad (2.11a)$$

$$\mathbf{K}(\mathbf{X}) \geq \mathbf{0}, \quad \mathbf{G}(\mathbf{X}) \geq \mathbf{0}, \quad \mathbf{K}(\mathbf{X}) \cdot \mathbf{G}(\mathbf{X}) = 0, \quad (2.11b)$$

155 where the linear operators  $\mathbf{K} : \mathbb{R}^n \rightarrow \mathbb{R}^m$  and  $\mathbf{G} : \mathbb{R}^n \rightarrow \mathbb{R}^m$  are defined as

$$\mathbf{G}(\mathbf{X}) := \mathbf{X}_1 - \mathbf{X}_2, \quad \text{and} \quad \mathbf{K}(\mathbf{X}) := \boldsymbol{\lambda}. \quad (2.12)$$

## 156 3 Semismooth Newton method

157 In this section, we consider the semismooth Newton linearization to approximate the solution of the nonlinear  
 158 system of equations (2.11), see, e.g., [27, 17].

159 The complementarity constraints (2.11b) written as algebraic inequalities can be expressed as a nonlinear  
 160 non-differentiable equality by means of C-functions, where C stands for complementarity. We say that a function  
 161  $\tilde{\mathbf{C}} : (\mathbb{R}^m)^2 \rightarrow \mathbb{R}^m$ ,  $m \geq 1$ , is a C-function if for any pair  $(\mathbf{x}, \mathbf{y}) \in (\mathbb{R}^m)^2$ ,

$$\tilde{\mathbf{C}}(\mathbf{x}, \mathbf{y}) = \mathbf{0} \iff \mathbf{x} \geq \mathbf{0}, \quad \mathbf{y} \geq \mathbf{0}, \quad \text{and} \quad \mathbf{x} \cdot \mathbf{y} = 0.$$

162 As examples, we consider the min and Fischer–Burmeister (F–B) functions

$$(\tilde{\mathbf{C}}_{\min}(\mathbf{x}, \mathbf{y}))_l := (\min\{\mathbf{x}, \mathbf{y}\})_l = (\mathbf{x}_l + \mathbf{y}_l)/2 - |\mathbf{x}_l - \mathbf{y}_l|/2 \quad l = 1, \dots, m, \quad (3.1)$$

$$(\tilde{\mathbf{C}}_{\text{FB}}(\mathbf{x}, \mathbf{y}))_l := \sqrt{\mathbf{x}_l^2 + \mathbf{y}_l^2} - (\mathbf{x}_l + \mathbf{y}_l) \quad l = 1, \dots, m. \quad (3.2)$$

163 For more details on C-functions see [27, 28]. Let us consider a function  $\mathbf{C} : \mathbb{R}^n \rightarrow \mathbb{R}^m$  defined as  $\mathbf{C}(\mathbf{X}) :=$   
 164  $\tilde{\mathbf{C}}(\mathbf{K}(\mathbf{X}), \mathbf{G}(\mathbf{X}))$ , where  $\tilde{\mathbf{C}}$  is any C-function and  $\mathbf{K}(\cdot), \mathbf{G}(\cdot)$  are given in (2.12). This allows to conveniently  
 165 state constraints (2.11b) in an equality of the form  $\mathbf{C}(\mathbf{X}) = \mathbf{0}$ . Then, problem (2.11) can be equivalently  
 166 rewritten as a system of nonlinear algebraic equations: find a vector  $\mathbf{X} \in \mathbb{R}^n$  such that

$$\mathbb{E}\mathbf{X} = \mathbf{F}, \quad (3.3a)$$

$$\mathbf{C}(\mathbf{X}) = \mathbf{0}. \quad (3.3b)$$

167 Note, however, that in general C-functions are not Fréchet-differentiable everywhere.

168 Next, we detail the semismooth Newton linearization of problem (3.3). Let an initial vector  $\mathbf{X}^0 \in \mathbb{R}^n$  be  
 169 given. At the step  $k \geq 1$ , one looks for  $\mathbf{X}^k \in \mathbb{R}^n$  such that

$$\mathbb{A}^{k-1} \mathbf{X}^k = \mathbf{B}^{k-1}, \quad (3.4)$$

170 where the Jacobian matrix  $\mathbb{A}^{k-1} \in \mathbb{R}^{n,n}$  and the right-hand side vector  $\mathbf{B}^{k-1} \in \mathbb{R}^n$  are given by

$$\mathbb{A}^{k-1} := \begin{bmatrix} \mathbb{E} \\ \mathbb{J}_{\mathbf{C}}(\mathbf{X}^{k-1}) \end{bmatrix}, \quad \mathbf{B}^{k-1} := \begin{bmatrix} \mathbf{F} \\ \mathbb{J}_{\mathbf{C}}(\mathbf{X}^{k-1})\mathbf{X}^{k-1} - \mathbf{C}(\mathbf{X}^{k-1}) \end{bmatrix}. \quad (3.5)$$

171 We emphasize that equation (3.3a) is linear and a semismooth nonlinearity occurs in the second line (3.3b). In  
 172 (3.5),  $\mathbb{J}_{\mathbf{C}}(\mathbf{X}^{k-1})$  stands for the Jacobian matrix in the sense of Clarke of the semismooth function  $\mathbf{C}$  at point  
 173  $\mathbf{X}^{k-1}$ , cf. [27, 28]. To give an example, we consider the semismooth min function (3.1) at  $\mathbf{X}^{k-1}$

$$\mathbf{C}(\mathbf{X}^{k-1}) = \min\{\mathbf{X}_1^{k-1} - \mathbf{X}_2^{k-1}, \boldsymbol{\lambda}^{k-1}\} = \min \left\{ \begin{pmatrix} u_{1,K_1}^{k-1} - u_{2,K_1}^{k-1} \\ \vdots \\ u_{1,K_m}^{k-1} - u_{2,K_m}^{k-1} \end{pmatrix}, \begin{pmatrix} \lambda_{K_1}^{k-1} \\ \vdots \\ \lambda_{K_m}^{k-1} \end{pmatrix} \right\}.$$

174 We define the block matrices  $\mathbb{G}$  and  $\mathbb{K} \in \mathbb{R}^{m,n}$  by  $\mathbb{G} = [\mathbb{I}_{m \times m}, -\mathbb{I}_{m \times m}, \mathbf{0}_{m \times m}]$  and  $\mathbb{K} = [\mathbf{0}_{m \times m}, \mathbf{0}_{m \times m}, \mathbb{I}_{m \times m}]$ .  
 175 Then, the  $l^{\text{th}}$  row of the Jacobian matrix in the sense of Clarke  $\mathbb{J}_{\mathbf{C}}(\mathbf{X}^{k-1})$  is either given by the  $l^{\text{th}}$  row of  $\mathbb{G}$ ,  
 176 if  $u_{1,K_l}^{k-1} - u_{2,K_l}^{k-1} \leq \lambda_{K_l}^{k-1}$ , or by the  $l^{\text{th}}$  row of  $\mathbb{K}$ , if  $\lambda_{K_l}^{k-1} < u_{1,K_l}^{k-1} - u_{2,K_l}^{k-1}$ .

## 177 4 Inexact smoothing Newton method

178 We now address the numerical approximation of the nonsmooth nonlinear problem (3.3) employing a smoothing  
 179 approach.

### 180 4.1 Discrete smoothed problem

181 We replace  $\mathbf{C}(\cdot)$  in problem (3.3) by a smoothed C-function  $\mathbf{C}_\mu(\cdot)$  of class  $\mathcal{C}^1$ , where  $\mu > 0$  is a (small) smoothing  
 182 parameter. A possible smoothing of the functions (3.1) and (3.2) can be, respectively: for  $l = 1, \dots, m$ ,

$$(\tilde{\mathbf{C}}_{\min_\mu}(\mathbf{x}, \mathbf{y}))_l = \frac{\mathbf{x}_l + \mathbf{y}_l}{2} - \frac{(|\mathbf{x} - \mathbf{y}|_\mu)_l}{2} \quad \text{with } (|\mathbf{z}|_\mu)_l := \sqrt{\mathbf{z}_l^2 + \mu^2}, \quad (4.1)$$

$$(\tilde{\mathbf{C}}_{\text{FB}_\mu}(\mathbf{x}, \mathbf{y}))_l = \sqrt{\mu^2 + \mathbf{x}_l^2 + \mathbf{y}_l^2} - (\mathbf{x}_l + \mathbf{y}_l), \quad (4.2)$$

183 where the  $\mu$ -smoothed absolute value function  $|\cdot|_\mu : \mathbb{R}^m \rightarrow \mathbb{R}_+^m$ ,  $m \geq 0$ , replaces the absolute value function  
 184 (not differentiable at  $\mathbf{0}$ ). Note that both functions  $\tilde{\mathbf{C}}_{\min,\mu}$  and  $\tilde{\mathbf{C}}_{\text{FB},\mu}$  are of class  $\mathcal{C}^\infty$ .

186 We now introduce a smoothing loop with index  $j \geq 1$ , where  $\mu_j > 0$  is a (decreasing) sequence of smoothing  
 187 parameters. The discrete smoothed problem at each outer smoothing step  $j \geq 1$  then reads as follows: find

188  $\mathbf{X}^j \in \mathbb{R}^n$  such that

$$\begin{aligned} \mathbb{E}\mathbf{X}^j &= \mathbf{F}, \\ \mathbf{C}_{\mu^j}(\mathbf{X}^j) &= \mathbf{0}, \end{aligned} \quad (4.3)$$

189 with  $\mathbf{C}_{\mu^j}(\mathbf{X}^j) := \tilde{\mathbf{C}}_{\mu^j}(\mathbf{K}(\mathbf{X}^j), \mathbf{G}(\mathbf{X}^j))$ . This approach gives rise to the nonlinear algebraic system (4.3) at  
 190 each smoothing step  $j \geq 1$ , which is differentiable. Its solution is approximated employing the (inexact) Newton  
 191 method detailed next.

## 192 4.2 Newton linearization

193 Let  $j \geq 1$  be fixed and let  $\mathbf{X}^{j,0}$  be a given initial vector. At each linearization iteration  $k \geq 1$ , the new  
 194 approximation  $\mathbf{X}^{j,k} \in \mathbb{R}^n$  is obtained solving the linear problem written as

$$\mathbb{A}_{\mu^j}^{j,k-1} \mathbf{X}^{j,k} = \mathbf{B}_{\mu^j}^{j,k-1}, \quad (4.4)$$

195 where the Jacobian matrix  $\mathbb{A}_{\mu^j}^{j,k-1} \in \mathbb{R}^{n,n}$  and the right-hand side vector  $\mathbf{B}_{\mu^j}^{j,k-1} \in \mathbb{R}^n$  are defined by

$$\mathbb{A}_{\mu^j}^{j,k-1} := \left[ \begin{array}{c} \mathbb{E} \\ \mathbb{J}_{\mathbf{C}_{\mu^j}}(\mathbf{X}^{j,k-1}) \end{array} \right], \quad \mathbf{B}_{\mu^j}^{j,k-1} := \left[ \begin{array}{c} \mathbf{F} \\ \mathbb{J}_{\mathbf{C}_{\mu^j}}(\mathbf{X}^{j,k-1})\mathbf{X}^{j,k-1} - \mathbf{C}_{\mu^j}(\mathbf{X}^{j,k-1}) \end{array} \right], \quad (4.5)$$

196 with  $\mathbb{J}_{\mathbf{C}_{\mu^j}}(\mathbf{X}^{j,k-1})$  the standard Jacobian matrix of the smooth function  $\mathbf{C}_{\mu^j}$  at  $\mathbf{X}^{j,k-1}$ .

## 197 4.3 Algebraic resolution

198 The system of linear algebraic equations (4.4) is typically numerically addressed using an iterative algebraic  
 199 solver. For a fixed smoothing step  $j \geq 1$ , a fixed Newton step  $k \geq 1$ , and a given initial vector  $\mathbf{X}^{j,k,0}$   
 200 (typically,  $\mathbf{X}^{j,k,0} = \mathbf{X}^{j,k-1,i}$ , the last iterate available from the previous linearization step), the iterative solver  
 201 generates for  $i \geq 1$  (inner loop in  $k$ ) a sequence  $\mathbf{X}^{j,k,i}$  approximating  $\mathbf{X}^{j,k}$  from (4.4) up to the residual given  
 202 by

$$\mathbf{R}_{\text{alg}}^{j,k,i} := \mathbf{B}_{\mu^j}^{j,k-1} - \mathbb{A}_{\mu^j}^{j,k-1} \mathbf{X}^{j,k,i}. \quad (4.6)$$

203 Detailing the first two equations of (4.6), we obtain for  $\alpha \in \{1, 2\}$ , at smoothing iteration  $j \geq 1$ , Newton  
 204 iteration  $k \geq 1$ , and linear solver iteration  $i \geq 1$ , the residual  $\mathbf{R}_{\text{alg},\alpha,K}^{j,k,i}$  given by

$$\left( \mathbf{R}_{\text{alg},\alpha}^{j,k,i} \right)_K := |K| f_{\alpha,K} - \sum_{\sigma \in \mathcal{E}_K} F_{\alpha,K,\sigma}^{j,k,i} - (-1)^\alpha |K| \lambda_K^{j,k,i}, \quad (4.7)$$

205 where  $\mathbf{R}_{\text{alg},\alpha,K}^{j,k,i}$  is the algebraic residual associated to the element  $K \in \mathcal{T}_h$ ,  $\alpha \in \{1, 2\}$ , and  $F_{\alpha,K,\sigma}^{j,k,i}$  is given by

$$F_{\alpha,K,\sigma}^{j,k,i} := \begin{cases} -\beta_\alpha |\sigma| \frac{u_{\alpha,L}^{j,k,i} - u_{\alpha,K}^{j,k,i}}{d_{K,L}} & \text{if } \sigma \in \mathcal{E}_h^{\text{int}}, \sigma = K \cap L, \\ -\beta_\alpha |\sigma| \frac{u_{\alpha,\sigma} - u_{\alpha,K}^{j,k,i}}{d_{K,\sigma}} & \text{if } \sigma \in \mathcal{E}_h^{\text{ext}}. \end{cases} \quad (4.8)$$

## 206 5 Postprocessing of the approximate solution and potential recon- 207 structions

208 This section introduces  $H^1(\Omega)$ -conforming reconstructed potentials that will be central in the formulation of  
 209 our posteriori error estimates.

### 210 5.1 Postprocessed potential

211 The discrete finite volume solution from (2.9) or more precisely from (4.6) is only piecewise constant, see Figure  
 212 1, left, for an illustration in one space dimension. Recall that it is defined for all  $K \in \mathcal{T}_h$  and  $\alpha \in \{1, 2\}$   
 213 by  $u_{\alpha h}^{j,k,i}|_K := u_{\alpha,K}^{j,k,i}$  and  $\lambda_h^{j,k,i}|_K := \lambda_K^{j,k,i}$ . In particular, setting  $\mathbf{u}_h^{j,k,i} := (u_{1h}^{j,k,i}, u_{2h}^{j,k,i})$ , the discrete solution is

214 such that

$$\begin{aligned} \mathbf{u}_h^{j,k,i} &\notin \mathcal{K}_g, \\ -\beta_\alpha \nabla u_{\alpha h}^{j,k,i} &\notin \mathbf{H}(\operatorname{div}, \Omega), \quad \alpha \in \{1, 2\}, \\ \nabla \cdot (-\beta_\alpha \nabla u_{\alpha h}^{j,k,i}) &\neq f_\alpha - (-1)^\alpha \lambda_h^{j,k,i}, \quad \alpha \in \{1, 2\}. \end{aligned}$$

215 In the subsequent sections, we try to mimic the above properties, satisfied by of the weak solution  $\mathbf{u}$ , by  
216 building reconstructions from the discrete approximate solution  $\mathbf{u}_h^{j,k,i}$ .

217 Let  $\mathbb{P}_p(K)$ ,  $p \geq 0$ , denote the set of polynomials of total degree at most  $p$  on the element  $K \in \mathcal{T}_h$ . First, to  
218 be able to evaluate the (broken) gradient of the approximate solution and to measure its distance to the exact  
219 solution by the energy (semi-)norm defined in (2.2), it is primordial to transform the piecewise constant solution  
220  $\mathbf{u}_h^{j,k,i}$  into a higher-order piecewise polynomial. To do so, we locally construct a postprocessed approximation  
221  $\tilde{\mathbf{u}}_h^{j,k,i}$  that lies in  $[\mathbb{P}_2(\mathcal{T}_h)]^2$ , the space of piecewise second-order polynomials, following [25, 56].

222 **Definition 5.1** (Postprocessed solution). *We introduce the piecewise quadratic, discontinuous, postprocessed*  
223 *solution  $\tilde{\mathbf{u}}_h^{j,k,i} := (\tilde{u}_{1h}^{j,k,i}, \tilde{u}_{2h}^{j,k,i}) \in [\mathbb{P}_2(\mathcal{T}_h)]^2$  as follows. Let  $F_{\alpha,K,\sigma}^{j,k,i}$  be given by (4.8). For  $\alpha \in \{1, 2\}$ , let*

$$\frac{(\tilde{u}_{\alpha h}^{j,k,i}, 1)_K}{|K|} = u_{\alpha,K}^{j,k,i}, \quad (5.1a)$$

$$-\beta_\alpha \nabla \tilde{u}_{\alpha h}^{j,k,i} \in (\mathbb{P}_0(K))^2 + x\mathbb{P}_0(K), \quad -\beta_\alpha \nabla \tilde{u}_{\alpha h}^{j,k,i} |_K \cdot \mathbf{n}_{K,\sigma} = \frac{F_{\alpha,K,\sigma}^{j,k,i}}{|\sigma|} \quad \forall \sigma \in \mathcal{E}_K. \quad (5.1b)$$

224 Figure 1, right part, gives an illustration of this postprocessed solution. Condition (5.1a) states that the  
225 mean value on each mesh element of the postprocessed solution is given by the original solution, whereas (5.1b)  
226 fixes the flux  $-\beta_\alpha \nabla \tilde{u}_{\alpha h}^{j,k,i}$  to be in the lowest-order Raviart–Thomas space and its normal component to coincide  
227 with the finite volume edge fluxes.

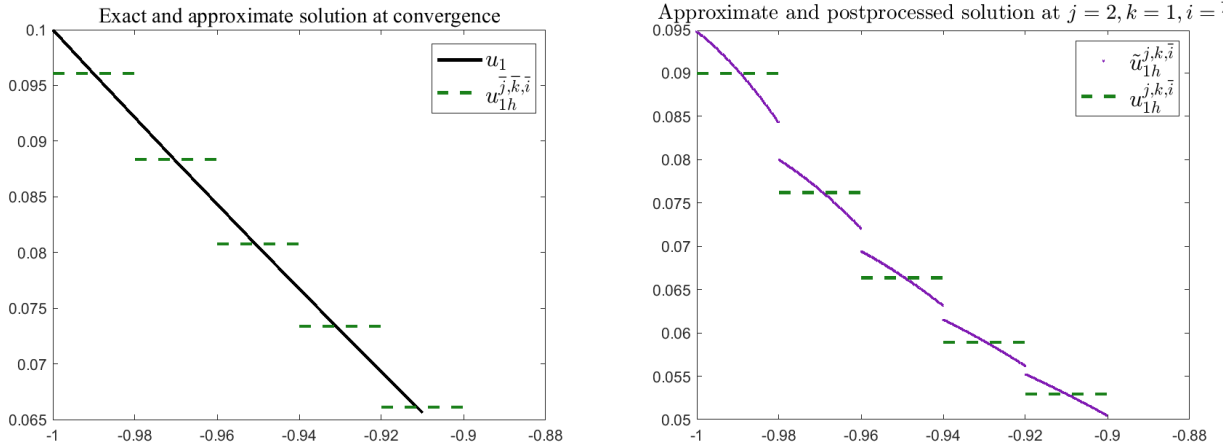


Figure 1: [Adaptive inexact smoothing Newton method, Algorithm 1, one space dimension, zoom on the first 5 elements of the computational mesh  $\mathcal{T}_h$ ] Left: exact solution  $u_1$  and approximate solution  $u_{1h}^{j,k,i}$  at convergence of all solvers. Right: Approximate solution  $u_{1h}^{j,k,i}$  and postprocessed solution  $\tilde{u}_{1h}^{j,k,i}$  at steps  $(j, k) = (2, 1)$  and at convergence of the algebraic solver ( $i = \bar{i}$ ).

## 228 5.2 Non-admissible potential reconstruction

229 The postprocessed solution  $\tilde{\mathbf{u}}_h^{j,k,i}$  of Definition 5.1 is not included in the convex space  $\mathcal{K}_g$ , already by the fact  
230 that it does not lie in  $H_g^1(\Omega) \times H_0^1(\Omega)$ . We will therefore introduce a continuous reconstructed solution  $\mathbf{s}_h$  that  
231 can still be nonphysical, in the sense that it may not satisfy the complementarity constraints, and thus not lie  
232 in  $\mathcal{K}_g$ , but at least it lies in  $H_g^1(\Omega) \times H_0^1(\Omega)$ .

233 **Notations.** Let  $X_h^p$ ,  $p \geq 1$ , stand for the discrete conforming space of piecewise polynomial functions

$$X_h^p := \{v_h \in C^0(\bar{\Omega}); v_h|_K \in \mathbb{P}_p(K), \forall K \in \mathcal{T}_h\} \subset H^1(\Omega). \quad (5.2)$$

234 We will in the sequel also need the boundary-aware set and space

$$X_{gh}^p := \{v_h \in X_h^p; v_h = g \text{ on } \partial\Omega\} \subset H_g^1(\Omega) \quad \text{and} \quad X_{0h}^p := X_h^p \cap H_0^1(\Omega) \subset H_0^1(\Omega). \quad (5.3)$$

235 **Definition 5.2** (Non-admissible potential reconstruction). We introduce  $\mathbf{s}_h^{j,k,i} := (s_{1h}^{j,k,i}, s_{2h}^{j,k,i})$ , given by, for  
236  $\alpha \in \{1, 2\}$ ,

$$\mathbf{s}_h^{j,k,i} := \mathcal{I}_{\text{Os}}(\tilde{\mathbf{u}}_h^{j,k,i}) := \left( \mathcal{I}_{\text{Os}}(\tilde{u}_{1h}^{j,k,i}), \mathcal{I}_{\text{Os}}(\tilde{u}_{2h}^{j,k,i}) \right), \quad (5.4)$$

237 where  $\mathcal{I}_{\text{Os}}$  denotes the Oswald interpolation operator previously considered in, e.g., [56]. This operator associates  
238 to the discontinuous piecewise polynomial  $\tilde{u}_{\alpha h}^{j,k,i}$ ,  $\alpha \in \{1, 2\}$ , its conforming interpolant, i.e., continuous and  
239 contained in  $H^1(\Omega)$ , by taking averages in all Lagrangian evaluation points and fixing the boundary values to  
240 respectively  $g$  or  $0$ . Figure 2 illustrates the postprocessed and the reconstructed solution at a specific smoothing  
241 and linearization iterations (left) and at convergence (right). The reconstructed solution is then piecewise second-  
242 order polynomial and continuous and satisfies

$$\mathbf{s}_h^{j,k,i} := (s_{1h}^{j,k,i}, s_{2h}^{j,k,i}) \in X_{gh}^2 \times X_{0h}^2 \subset H_g^1(\Omega) \times H_0^1(\Omega).$$

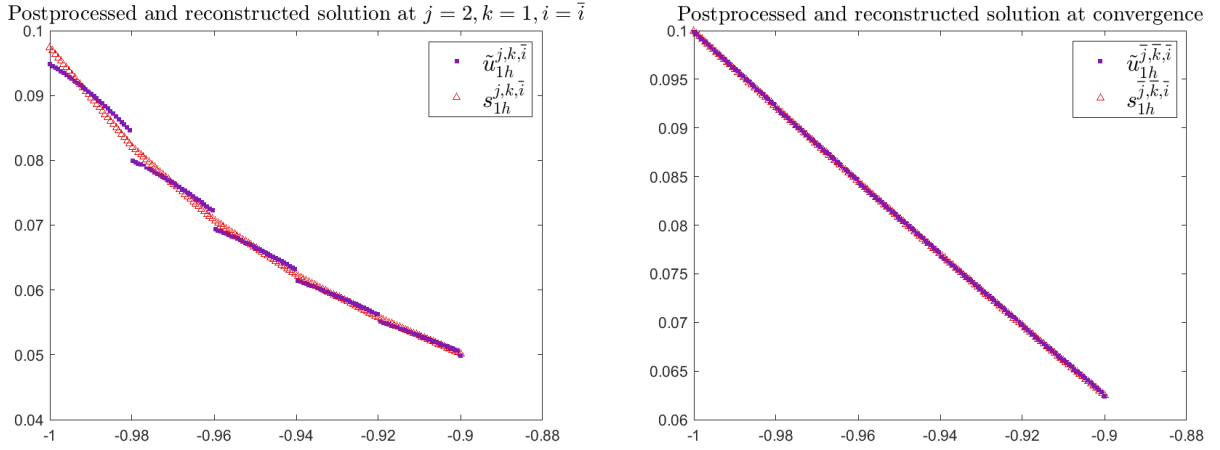


Figure 2: [Adaptive inexact smoothing Newton method, Algorithm 1, one space dimension, zoom on the first 5 elements of the computational mesh  $\mathcal{T}_h$ ] Postprocessed solution  $\tilde{u}_{1h}^{j,k,i}$  and reconstructed solution  $s_{1h}^{j,k,i}$  at steps  $(j, k) = (2, 1)$  and at convergence of the algebraic solver ( $i = \bar{i}$ ), left. Postprocessed solution  $\tilde{u}_{1h}^{j,k,i}$  and reconstructed solution  $s_{1h}^{j,k,i}$  at convergence of all solvers, right.

### 243 5.3 Admissible potential reconstruction

244 It may happen that the potential reconstruction  $\mathbf{s}_h^{j,k,i}$  defined by (5.4) violates the non-penetration condi-  
245 tion  $s_{1h}^{j,k,i} - s_{2h}^{j,k,i} \geq 0$ , see Figure 3, so that  $\mathbf{s}_h^{j,k,i} \notin \mathcal{K}_g$ , where we recall  $\mathcal{K}_g$  is given in (2.7). In order to  
246 avoid this, we build from the potential reconstruction  $\mathbf{s}_h^{j,k,i} \in X_{gh}^2 \times X_{0h}^2 \not\subset \mathcal{K}_g$ , a final admissible potential  
247 reconstruction  $\tilde{\mathbf{s}}_h^{j,k,i} \in \mathcal{K}_g$ ,  $\tilde{\mathbf{s}}_h^{j,k,i} \in X_{gh}^3 \times X_{0h}^3$ . We now provide details on how to build it.

248 **Definition 5.3** (Admissible potential reconstruction). We employ the following possible procedure, which is  
249 composed of two steps:

250 *Step 1.* First, we construct  $\hat{\mathbf{s}}_h^{j,k,i} \in X_{gh}^2 \times X_{0h}^2 \subset H_g^1(\Omega) \times H_0^1(\Omega)$  such that for each Lagrangian evaluation node  
251  $\mathbf{a}$

$$\hat{\mathbf{s}}_h^{j,k,i}(\mathbf{a}) := \begin{cases} \left( s_{1h}^{j,k,i}(\mathbf{a}), s_{2h}^{j,k,i}(\mathbf{a}) \right) & \text{if } s_{1h}^{j,k,i}(\mathbf{a}) \geq s_{2h}^{j,k,i}(\mathbf{a}), \\ \left( \frac{1}{2} \left( s_{1h}^{j,k,i}(\mathbf{a}) + s_{2h}^{j,k,i}(\mathbf{a}) \right), \frac{1}{2} \left( s_{1h}^{j,k,i}(\mathbf{a}) + s_{2h}^{j,k,i}(\mathbf{a}) \right) \right) & \text{if } s_{1h}^{j,k,i}(\mathbf{a}) < s_{2h}^{j,k,i}(\mathbf{a}). \end{cases} \quad (5.5)$$

252 Step 2. We point out that even if the inequality  $(\hat{s}_{1h}^{j,k,i} - \hat{s}_{2h}^{j,k,i})(\mathbf{a}) \geq 0$  is satisfied by the above first construction  
 253 step for all Lagrangian nodes  $\mathbf{a}$ , this does not necessarily imply that  $\hat{s}_{1h}^{j,k,i} \geq \hat{s}_{2h}^{j,k,i}$  everywhere, see the left part  
 254 of Figure 4. To guarantee the requested property, we proceed as follows:

255 a) First, go through all internal edges  $\sigma \in \mathcal{E}^{\text{int}}$  of the mesh  $\mathcal{T}_h$ . Consider the second-degree polynomial  
 256  $\hat{s}_\sigma := (\hat{s}_{1h}^{j,k,i} - \hat{s}_{2h}^{j,k,i})|_\sigma$  on the edge  $\sigma$ . If  $\hat{s}_\sigma \geq 0$ , i.e.  $\hat{s}_\sigma$  is nonnegative over  $\sigma$ , set  $c_\sigma := 0$ . Otherwise,  $\hat{s}_\sigma$   
 257 takes negative values inside  $\sigma$ . Let  $\omega_\sigma$  be the subdomain formed by the two triangles that share the edge  $\sigma$ .  
 258 Consider the edge bubble function  $\psi_\sigma$ , a non-negative piecewise second-order polynomial defined over  $\omega_\sigma$ ,  
 259 continuous over  $\sigma$ , zero on  $\partial\omega_\sigma$ , with  $\|\psi_\sigma\|_{\infty,\omega_\sigma} = 1$ . Let  $c_\sigma$  be the smallest positive constant such that  
 260  $(\hat{s}_\sigma + c_\sigma\psi_\sigma)|_\sigma \geq 0$  on  $\sigma$ .

261 b) Second, go through all elements  $K$  of  $\mathcal{T}_h$ . Consider the second-degree polynomial  $\hat{s}_K := (\hat{s}_{1h}^{j,k,i} - \hat{s}_{2h}^{j,k,i})|_K +$   
 262  $(\sum_{\sigma \in \mathcal{E}_K^{\text{int}}} c_\sigma\psi_\sigma)|_K$  on the triangle  $K$ . If  $\hat{s}_K \geq 0$ , set  $c_K := 0$ . Otherwise, consider the element bubble  
 263 function  $\psi_K$ , a non-negative third-order polynomial defined over  $K$ , zero on  $\partial K$ , with  $\|\psi_K\|_{\infty,K} = 1$ . Let  
 264  $c_K$  be the smallest positive constant such that  $\hat{s}_K + c_K\psi_K \geq 0$  on the element  $K$ .

265 c) The last step of our construction is to define  $\tilde{s}_h^{j,k,i}$ , for  $\alpha \in \{1, 2\}$ , by

$$\tilde{s}_{\alpha h}^{j,k,i} := \hat{s}_{\alpha h}^{j,k,i} - (-1)^\alpha \frac{1}{2} \sum_{\sigma \in \mathcal{E}_h^{\text{int}}} c_\sigma \psi_\sigma - (-1)^\alpha \frac{1}{2} \sum_{K \in \mathcal{T}_h} c_K \psi_K. \quad (5.6)$$

266 This yields

$$\tilde{s}_h^{j,k,i} \in X_{gh}^3 \times X_{0h}^3 \subset H_g^1(\Omega) \times H_0^1(\Omega), \quad \text{with } \tilde{s}_{1h}^{j,k,i} \geq \tilde{s}_{2h}^{j,k,i},$$

267 so that

$$\tilde{s}_h^{j,k,i} \in \mathcal{K}_g.$$

268 An illustration of the two steps described above is given in Figure 4.

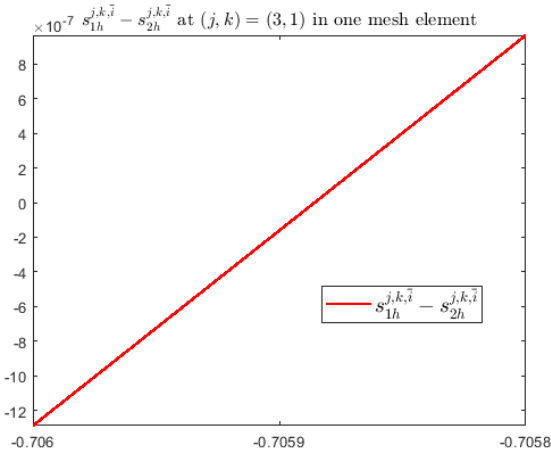


Figure 3: [Adaptive inexact smoothing Newton method, Algorithm 1, one space dimension, zoom on one element of the computational mesh  $\mathcal{T}_h$ ]  $s_{1h}^{j,k,\bar{i}} - s_{2h}^{j,k,\bar{i}}$  at steps  $(j, k) = (3, 1)$ , at convergence of the algebraic solver ( $i = \bar{i}$ ).

## 269 6 Flux reconstructions

270 We present in this section a construction of an equilibrated flux  $\tilde{\sigma}_{\alpha h}^{j,k,i}$  providing a discrete approximation of the  
 271 exact flux  $-\beta_\alpha \nabla u_\alpha$ , cf. [56]. For this purpose, we will need the lowest-order Raviart–Thomas finite-dimensional  
 272 subspace of  $\mathbf{H}(\text{div}, \Omega)$ , defined by

$$\mathbf{RT}_0(\Omega) := \{\mathbf{v}_h \in \mathbf{H}(\text{div}, \Omega); \mathbf{v}_h|_K \in [\mathbb{P}_0(K)]^2 + \mathbf{x}\mathbb{P}_0(K)\}, \quad \forall K \in \mathcal{T}_h.$$

273 In particular,  $\mathbf{v}_h \in \mathbf{RT}_0(\Omega)$  is such that  $(\nabla \cdot \mathbf{v}_h)|_K \in \mathbb{P}_0(K), \forall K \in \mathcal{T}_h$ , and  $(\mathbf{v}_h \cdot \mathbf{n})|_\sigma \in \mathbb{P}_0(\sigma), \forall \sigma \in \mathcal{E}_K$ . For  
 274 more details, we refer to [14].

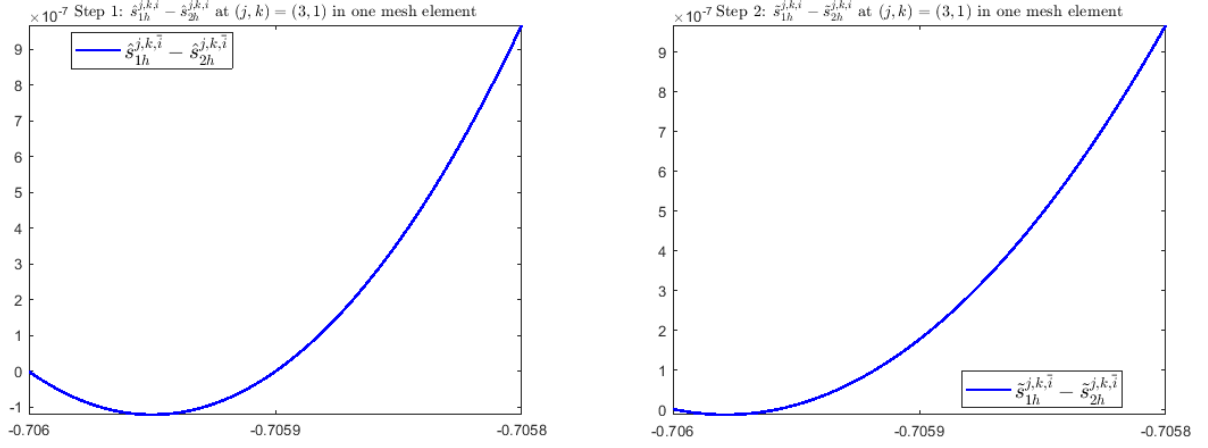


Figure 4: [Adaptive inexact smoothing Newton method, Algorithm 1, one space dimension, zoom on one element of the computational mesh  $\mathcal{T}_h$ ]  $\hat{s}_{1h}^{j,k,i} - \hat{s}_{2h}^{j,k,i}$  after the reconstruction step 1, left, and  $\tilde{s}_{1h}^{j,k,i} - \tilde{s}_{2h}^{j,k,i}$  after the reconstruction step 2, right, at steps  $(j, k) = (3, 1)$  and at convergence of the algebraic solver ( $i = i$ ).

Let  $\Pi_{\mathbb{P}_0}$  denote the  $L_2(\Omega)$ -orthogonal projection onto  $\mathbb{P}_0(\mathcal{T}_h)$ , the space of piecewise constants. An equilibrated flux reconstruction  $\tilde{\sigma}_{\alpha h}^{j,k,i}$  is a piecewise vector-valued polynomial function, designed to approximate  $\sigma_\alpha = -\beta_\alpha \nabla u_\alpha$ , and satisfying

$$\tilde{\sigma}_{\alpha h}^{j,k,i} \in \mathbf{RT}_0(\Omega), \quad (6.1a)$$

$$\nabla \cdot \tilde{\sigma}_{\alpha h}^{j,k,i} = \Pi_{\mathbb{P}_0}(f_\alpha) - (-1)^\alpha \lambda_h^{j,k,i} \in \mathbb{P}_0(\mathcal{T}_h). \quad (6.1b)$$

The remaining difference between  $f_\alpha$  and  $\Pi_{\mathbb{P}_0}(f_\alpha)$  will be considered in the next section, giving rise to the so-called data oscillation. Note that the reconstructed flux mimics the properties of the weak flux. Indeed, (6.1b) is a discrete form of the condition  $\nabla \cdot \sigma_\alpha = f_\alpha - (-1)^\alpha \lambda$ , where only the mean values of the divergence of  $\tilde{\sigma}_{\alpha h}^{j,k,i}$  need to coincide with the mean values of  $f_\alpha$  on each mesh element. This can equivalently be written as

$$\left( \nabla \cdot \tilde{\sigma}_{\alpha h}^{j,k,i} + (-1)^\alpha \lambda_h^{j,k,i}, 1 \right)_K = (f_\alpha, 1)_K, \quad \forall K \in \mathcal{T}_h.$$

We would like to emphasize that since the construction of the fluxes is based on the first two diffusion equations in (1.6) that are linear, there is no need to construct any linearization error flux as in [22]. To cope with inexact algebraic solver, though, we define the algebraic error flux reconstruction as follows.

**Definition 6.1** (Algebraic error flux reconstruction). *Let the smoothing step  $j \geq 1$ , the step of the nonlinear solver  $k \geq 1$ , and the step of the linear solver  $i \geq 1$  be fixed. Given  $\mathbf{R}_{\text{alg},\alpha,K}^{j,k,i}$  defined in (4.7), and following [44, Concept 4.1], we can define the algebraic error flux reconstruction  $\tilde{\sigma}_{\alpha h,\text{alg}}^{j,k,i}$  in  $\mathbf{RT}_0(\mathcal{T}_h)$  for  $\alpha \in \{1, 2\}$  as follows*

$$\nabla \cdot \tilde{\sigma}_{\alpha h,\text{alg}}^{j,k,i}|_K = \frac{\mathbf{R}_{\text{alg},\alpha,K}^{j,k,i}}{|K|}, \quad \forall K \in \mathcal{T}_h. \quad (6.2)$$

**Definition 6.2** (Total flux reconstruction). *The total flux reconstruction  $\tilde{\sigma}_{\alpha h}^{j,k,i} \in \mathbf{RT}_0(\mathcal{T}_h)$  is defined by*

$$\tilde{\sigma}_{\alpha h}^{j,k,i} := -\beta_\alpha \nabla \tilde{u}_{\alpha h}^{j,k,i} + \tilde{\sigma}_{\alpha h,\text{alg}}^{j,k,i}. \quad (6.3)$$

**Lemma 6.3** (Total flux reconstruction). *There holds (6.1).*

*Proof.* First, condition (6.1a) follows from Definition 5.1 of the postprocessed solution together with Definition

291 **6.1.** To show (6.1b), we apply the Green formula and then employ (5.1b) and (4.7) which shows

$$\begin{aligned}
\left(\nabla \cdot \tilde{\boldsymbol{\sigma}}_{\alpha h}^{j,k,i}, 1\right)_K &= \left(\nabla \cdot (-\beta_\alpha \nabla \tilde{\mathbf{u}}_{\alpha h}^{j,k,i}) + \nabla \cdot \tilde{\boldsymbol{\sigma}}_{\alpha h, \text{alg}}^{j,k,i}, 1\right)_K \\
&= \sum_{\sigma \in \mathcal{E}_K} \left(-\beta_\alpha \nabla \tilde{\mathbf{u}}_{\alpha h}^{j,k,i} \cdot \mathbf{n}_{K,\sigma}, 1\right)_\sigma + \left(\nabla \cdot \tilde{\boldsymbol{\sigma}}_{\alpha h, \text{alg}}^{j,k,i}, 1\right)_K \\
&\stackrel{(5.1b), (6.2)}{=} \sum_{\sigma \in \mathcal{E}_K} F_{\alpha, K, \sigma}^{j,k,i} + \mathbf{R}_{\text{alg}, \alpha, K}^{j,k,i} \\
&\stackrel{(4.7)}{=} \left(f_{\alpha, K} - (-1)^\alpha \lambda_K^{j,k,i}, 1\right)_K.
\end{aligned}$$

292

□

293 **Remark 6.4** (Practical approximate algebraic error flux reconstruction). We use below a simple and practical  
294 approach to approximate the algebraic error flux reconstruction  $\tilde{\boldsymbol{\sigma}}_{\alpha h, \text{alg}}^{j,k,i}$ , following [22, Section 4]. Let  $\nu > 0$  be  
295 a user-given fixed parameter. Performing  $\nu$  additional steps of the linear solver, then computing  $-\beta_\alpha \nabla \tilde{\mathbf{u}}_{\alpha h}^{j,k,i+\nu}$   
296 as in (5.1b) with  $i + \nu$  in place of  $i$ , an algebraic error flux reconstruction can be defined as

$$\tilde{\boldsymbol{\sigma}}_{\alpha h, \text{alg}}^{j,k,i} := -\beta_\alpha \nabla \tilde{\mathbf{u}}_{\alpha h}^{j,k,i+\nu} - \left(-\beta_\alpha \nabla \tilde{\mathbf{u}}_{\alpha h}^{j,k,i}\right),$$

297 satisfying (6.2) approximately.

## 298 7 A posteriori error estimates

299 Equipped with the key ingredients of the a posteriori analysis, namely the postprocessing and reconstructions  
300 of Sections 5 and 6, we are now in a position to rigorously derive an a posteriori estimate for the displacements.  
301 This allows to obtain a fully computable error upper bound at any smoothing step  $j \geq 1$ , any linearization step  
302  $k \geq 1$ , and any step of the algebraic solver  $i \geq 1$  of the inexact smoothing Newton method of Section 4. Let us  
303 stress that, for  $j \geq 1, k \geq 1$ , and  $i \geq 1$ , the conditions  $(u_{1h}^{j,k,i} - u_{2h}^{j,k,i}) \geq 0$ ,  $\lambda_h^{j,k,i} \geq 0$ , and  $\lambda_h^{j,k,i}(u_{1h}^{j,k,i} - u_{2h}^{j,k,i}) = 0$   
304 are not necessarily satisfied, see Figure 5 for an illustration. In addition to the developments of Section 5, to  
305 deal with the possible violation of condition  $\lambda_h^{j,k,i} \geq 0$ , we define the negative and positive parts of  $\lambda_h^{j,k,i}$  by

$$\lambda_h^{j,k,i} = \lambda_h^{j,k,i,\text{pos}} + \lambda_h^{j,k,i,\text{neg}}, \quad \lambda_h^{j,k,i,\text{pos}} := \max\{\lambda_h^{j,k,i}, 0\}, \quad \lambda_h^{j,k,i,\text{neg}} := \min\{\lambda_h^{j,k,i}, 0\}.$$

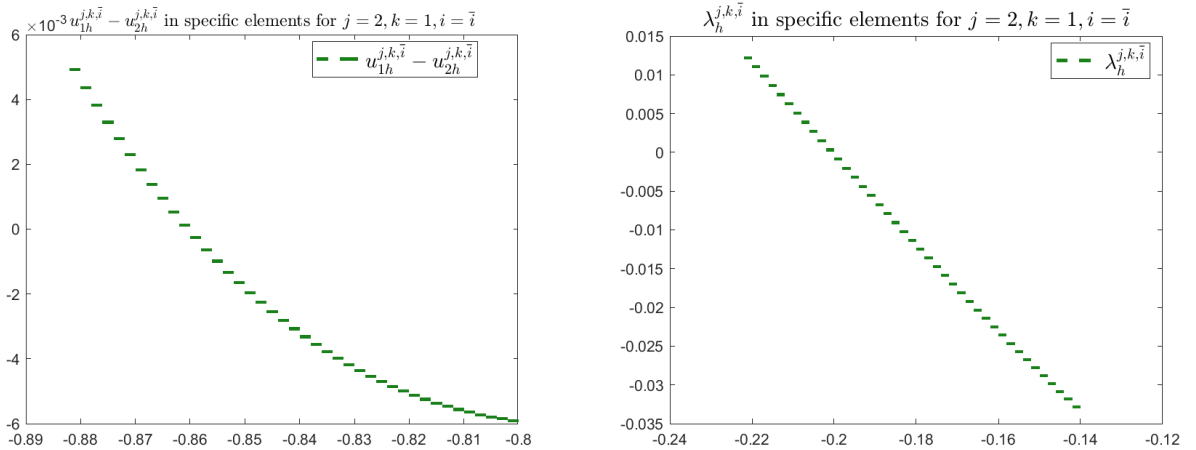


Figure 5: [Adaptive inexact smoothing Newton method, Algorithm 1, one space dimension, zoom on some elements of the computational mesh  $\mathcal{T}_h$ ]  $u_{1h}^{j,k,i} - u_{2h}^{j,k,i}$ , left, and  $\lambda_h^{j,k,i}$ , right, in specific elements, at steps  $(j, k) = (2, 1)$  and at convergence of the algebraic solver ( $i = \bar{i}$ ).

## 7.1 A posteriori error estimate for the displacements

Recall that  $C_{\text{PF}}$  and  $C_{\text{PW}}$  are the Poincaré constants from (2.1). Let  $C_{\beta,\Omega} := C_{\text{PF}}h_{\Omega}(\frac{1}{\beta_1} + \frac{1}{\beta_2})^{\frac{1}{2}}$ . We introduce for each element different estimators  $\eta_{\cdot,K}^{j,k,i}, K \in \mathcal{T}_h$  together with their global counterparts  $\eta^{j,k,i} := \{\sum_{K \in \mathcal{T}_h} (\eta_{\cdot,K}^{j,k,i})^2\}^{\frac{1}{2}}$ . We then have the following theorem.

**Theorem 7.1** (A posteriori estimate for the displacements). *Let  $\mathbf{u} \in \mathcal{K}_g$  be the weak solution of (2.8). Consider the finite volume discretization (4.7)–(4.8) on smoothing step  $j \geq 1$ , linearization step  $k \geq 1$ , and algebraic step  $i \geq 1$ . Let the postprocessed solution  $\tilde{\mathbf{u}}_h^{j,k,i}$  be given following Definition 5.1, and the admissible potential reconstruction  $\tilde{\mathbf{s}}_h^{j,k,i}$  following Definition 5.3. Next, let the algebraic error flux reconstruction be given following Definition 6.1, and the total flux reconstruction following Definition 6.2. Let  $\Pi_0^\sigma$  be the  $L^2(\sigma)$ -orthogonal projection onto constants. For  $\alpha \in \{1, 2\}$ , define the local elementwise estimators*

$$\eta_{\text{nonc},K}^{j,k,i} := \left\| \tilde{\mathbf{s}}_h^{j,k,i} - \tilde{\mathbf{u}}_h^{j,k,i} \right\|_K, \quad (7.1a)$$

$$\eta_{\text{osc},K,\alpha} := C_{\text{PW}}h_K\beta_\alpha^{-\frac{1}{2}} \|f_\alpha - \Pi_{\mathbb{P}_0}(f_\alpha)\|_K, \quad \eta_{\text{osc}} := \left( \sum_{K \in \mathcal{T}_h} \sum_{\alpha=1}^2 (\eta_{\text{osc},K,\alpha})^2 \right)^{\frac{1}{2}}, \quad (7.1b)$$

$$\eta_{\text{alg},K,\alpha}^{j,k,i} := \beta_\alpha^{-\frac{1}{2}} \left\| \tilde{\boldsymbol{\sigma}}_{\alpha h, \text{alg}}^{j,k,i} \right\|_K, \quad \eta_{\text{alg}}^{j,k,i} := \left( \sum_{K \in \mathcal{T}_h} \sum_{\alpha=1}^2 (\eta_{\text{alg},K,\alpha}^{j,k,i})^2 \right)^{\frac{1}{2}}, \quad (7.1c)$$

$$\eta_{\text{sm,lin,alg},1,K}^{j,k,i} := C_{\beta,\Omega} \left\| \lambda_h^{j,k,i,\text{neg}} \right\|_K, \quad \eta_{\text{sm,lin,alg},2,K}^{j,k,i} := 2 \left( \lambda_h^{j,k,i,\text{pos}}, \tilde{\mathbf{s}}_{1h}^{j,k,i} - \tilde{\mathbf{s}}_{2h}^{j,k,i} \right)_K. \quad (7.1d)$$

Then, defining the total estimator by

$$\eta^{j,k,i} := \left\{ \left( \eta_{\text{osc}} + \eta_{\text{alg}}^{j,k,i} + \eta_{\text{nonc}}^{j,k,i} + \eta_{\text{sm,lin,alg},1}^{j,k,i} \right)^2 + \sum_{K \in \mathcal{T}_h} \eta_{\text{sm,lin,alg},2,K}^{j,k,i} \right\}^{\frac{1}{2}}, \quad (7.2)$$

the following a posteriori error estimate holds for the energy semi-norm, as well as for the energy semi-norm augmented by the jump term for the the postprocessed solution

$$\left\| \mathbf{u} - \tilde{\mathbf{u}}_h^{j,k,i} \right\| \leq \eta^{j,k,i}, \quad (7.3a)$$

$$\left\| \mathbf{u} - \tilde{\mathbf{u}}_h^{j,k,i} \right\| + \left\{ \sum_{\sigma \in \mathcal{E}_h} |\sigma|^{-1} \left\| \left[ \mathbf{u} - \Pi_0^\sigma(\tilde{\mathbf{u}}_h^{j,k,i}) \right] \right\|_\sigma^2 \right\}^{\frac{1}{2}} \leq \eta^{j,k,i} + \left\{ \sum_{\sigma \in \mathcal{E}_h} |\sigma|^{-1} \left\| \left[ \Pi_0^\sigma(\tilde{\mathbf{u}}_h^{j,k,i}) \right] \right\|_\sigma^2 \right\}^{\frac{1}{2}}. \quad (7.3b)$$

**Remark 7.2** (Estimates (7.3)). *The estimate (7.3a) gives a fully computable upper bound on the energy semi-norm of the error between the exact solution  $\mathbf{u}$  and its approximation  $\tilde{\mathbf{u}}_h^{j,k,i}$  at each smoothing, linearization, and algebraic iterations  $j, k$ , and  $i \geq 1$ . The data oscillation estimators  $\eta_{\text{osc},K,\alpha}$  come from the fact that the source term is not necessarily piecewise constant, whereas  $\eta_{\text{alg},K,\alpha}^{j,k,i}$  reflect the algebraic error. The estimators  $\eta_{\text{sm,lin,alg},1,K}^{j,k,i}$  and  $\eta_{\text{sm,lin,alg},2,K}^{j,k,i}$  reflect inconsistencies in the contact conditions at the discrete level, whereas  $\eta_{\text{nonc},K}^{j,k,i}$  evaluates the nonconformity of the postprocessed solution  $\tilde{\mathbf{u}}_h^{j,k,i}$ , i.e. the fact that it does not lie in  $\mathcal{K}_g$ . Finally, (7.3b) adds an error jump term to the left which equals the jump estimator on the right since  $[[u_\alpha]] = 0, \alpha \in \{1, 2\}$ . This transforms the energy semi-norm into a norm.*

*Proof.* We first remark that (7.3b) follows from (7.3a) by adding to both sides of the inequality the same term, since  $[[\mathbf{u}]] = 0$ . To prove (7.3a), we distinguish the following two cases.

**Case 1.** If  $\left\| \mathbf{u} - \tilde{\mathbf{u}}_h^{j,k,i} \right\| \leq \left\| \mathbf{u} - \tilde{\mathbf{s}}_h^{j,k,i} \right\|$ , we just have to estimate  $\left\| \mathbf{u} - \tilde{\mathbf{s}}_h^{j,k,i} \right\|$ .

The reduced problem (2.8) for the test function  $\mathbf{v} = \tilde{\mathbf{s}}_h^{j,k,i} \in \mathcal{K}_g$  gives

$$a(\mathbf{u}, \mathbf{u} - \tilde{\mathbf{s}}_h^{j,k,i}) \leq l(\mathbf{u} - \tilde{\mathbf{s}}_h^{j,k,i}). \quad (7.4)$$

Denoting  $\mathbf{w} := \mathbf{u} - \tilde{\mathbf{s}}_h^{j,k,i}$ , we use (7.4) and add and subtract  $a(\tilde{\mathbf{u}}_h^{j,k,i}, \mathbf{w})$  and  $b(\mathbf{w}, \lambda_h^{j,k,i})$  to get, also employing

333 the notations (2.4),

$$\begin{aligned}
a(\mathbf{w}, \mathbf{w}) &\leq l(\mathbf{w}) + b(\mathbf{w}, \lambda_h^{j,k,i}) - a(\tilde{\mathbf{u}}_h^{j,k,i}, \mathbf{w}) + a(\tilde{\mathbf{u}}_h^{j,k,i} - \tilde{\mathbf{s}}_h^{j,k,i}, \mathbf{w}) - b(\mathbf{w}, \lambda_h^{j,k,i}) \\
&= \sum_{\alpha=1}^2 \left( f_\alpha - (-1)^\alpha \lambda_h^{j,k,i}, w_\alpha \right) - \sum_{\alpha=1}^2 \beta_\alpha \left( \nabla \tilde{\mathbf{u}}_{\alpha h}^{j,k,i}, \nabla w_\alpha \right) + a(\tilde{\mathbf{u}}_h^{j,k,i} - \tilde{\mathbf{s}}_h^{j,k,i}, \mathbf{w}) - b(\mathbf{w}, \lambda_h^{j,k,i}).
\end{aligned} \tag{7.5}$$

334 As  $\tilde{\boldsymbol{\sigma}}_{\alpha h}^{j,k,i} \in \mathbf{H}(\operatorname{div}, \Omega)$  by (6.1a), and as, relying on Definition 5.3,  $w_\alpha \in H_0^1(\Omega)$ , the Green formula gives

$$\left( \nabla \cdot \tilde{\boldsymbol{\sigma}}_{\alpha h}^{j,k,i}, w_\alpha \right) = - \left( \tilde{\boldsymbol{\sigma}}_{\alpha h}^{j,k,i}, \nabla w_\alpha \right) \quad \forall \alpha \in \{1, 2\}. \tag{7.6}$$

335 Then, from (6.3) and (7.6), we have

$$\begin{aligned}
a(\mathbf{w}, \mathbf{w}) &\leq \sum_{\alpha=1}^2 \sum_{K \in \mathcal{T}_h} \left( f_\alpha - (-1)^\alpha \lambda_h^{j,k,i} - \nabla \cdot \tilde{\boldsymbol{\sigma}}_{\alpha h}^{j,k,i}, w_\alpha \right)_K - \sum_{\alpha=1}^2 \sum_{K \in \mathcal{T}_h} \left( \tilde{\boldsymbol{\sigma}}_{\alpha h, \text{alg}}^{j,k,i}, \nabla w_\alpha \right)_K \\
&\quad + a(\tilde{\mathbf{u}}_h^{j,k,i} - \tilde{\mathbf{s}}_h^{j,k,i}, \mathbf{w}) - b(\mathbf{w}, \lambda_h^{j,k,i}).
\end{aligned} \tag{7.7}$$

337 It remains to bound each of the four terms in (7.7).

338 Using for the first term the flux property (6.1b) and the Cauchy–Schwarz and Poincaré–Wirtinger inequalities  
339 (2.1b) as  $w_\alpha|_K \in H^1(K)$ , we have

$$\begin{aligned}
\left( f_\alpha - (-1)^\alpha \lambda_h^{j,k,i} - \nabla \cdot \tilde{\boldsymbol{\sigma}}_{\alpha h}^{j,k,i}, w_\alpha \right)_K &= (f_\alpha - \Pi_{\mathbb{P}_0}(f_\alpha), w_\alpha - \bar{w}_{\alpha, K})_K \leq \eta_{\text{osc}, K, \alpha} \left\| \beta_\alpha^{\frac{1}{2}} \nabla w_\alpha \right\|_K, \\
\left( \tilde{\boldsymbol{\sigma}}_{\alpha h, \text{alg}}^{j,k,i}, \nabla w_\alpha \right)_K &\leq \eta_{\text{alg}, K, \alpha} \left\| \beta_\alpha^{\frac{1}{2}} \nabla w_\alpha \right\|_K,
\end{aligned}$$

341 where  $\bar{w}_{\alpha, K}$  denotes the mean value of  $w_\alpha$  on  $K$ . By applying the Cauchy–Schwarz inequality and using the  
342 definition of the energy semi-norm (2.2), we obtain

$$\sum_{\alpha=1}^2 \sum_{K \in \mathcal{T}_h} \left( f_\alpha - (-1)^\alpha \lambda_h^{j,k,i} - \nabla \cdot \tilde{\boldsymbol{\sigma}}_{\alpha h}^{j,k,i}, w_\alpha \right)_K \leq \eta_{\text{osc}} \left\| \mathbf{u} - \tilde{\mathbf{s}}_h^{j,k,i} \right\|, \tag{7.8}$$

343

$$- \sum_{\alpha=1}^2 \sum_{K \in \mathcal{T}_h} \left( \tilde{\boldsymbol{\sigma}}_{\alpha h, \text{alg}}^{j,k,i}, \nabla w_\alpha \right)_K \leq \eta_{\text{alg}}^{j,k,i} \left\| \mathbf{u} - \tilde{\mathbf{s}}_h^{j,k,i} \right\|. \tag{7.9}$$

344 For the third term of (7.7), applying the Cauchy–Schwarz inequality, we get

$$a(\tilde{\mathbf{u}}_h^{j,k,i} - \tilde{\mathbf{s}}_h^{j,k,i}, \mathbf{w}) \leq \underbrace{\left\| \tilde{\mathbf{u}}_h^{j,k,i} - \tilde{\mathbf{s}}_h^{j,k,i} \right\|}_{\eta_{\text{nonc}}^{j,k,i}} \left\| \mathbf{u} - \tilde{\mathbf{s}}_h^{j,k,i} \right\|. \tag{7.10}$$

345 Next, as  $\mathbf{u} \in \mathcal{K}_g$ ,  $-b(\mathbf{u}, \lambda_h^{j,k,i, \text{pos}}) \leq 0$ , and since  $\mathbf{w} = \mathbf{u} - \tilde{\mathbf{s}}_h^{j,k,i}$ , we have

$$-b(\mathbf{w}, \lambda_h^{j,k,i, \text{pos}}) \leq b(\tilde{\mathbf{s}}_h^{j,k,i}, \lambda_h^{j,k,i, \text{pos}}).$$

346 Using the fact that  $\lambda_h^{j,k,i} = \lambda_h^{j,k,i, \text{pos}} + \lambda_h^{j,k,i, \text{neg}}$ , the last term of (7.7) will be estimated as

$$-b(\mathbf{w}, \lambda_h^{j,k,i}) \leq -b(\mathbf{w}, \lambda_h^{j,k,i, \text{neg}}) + b(\tilde{\mathbf{s}}_h^{j,k,i}, \lambda_h^{j,k,i, \text{pos}}) \tag{7.11a}$$

$$= -(\lambda_h^{j,k,i, \text{neg}}, w_1 - w_2) + \left( \lambda_h^{j,k,i, \text{pos}}, \tilde{\mathbf{s}}_{1h}^{j,k,i} - \tilde{\mathbf{s}}_{2h}^{j,k,i} \right). \tag{7.11b}$$

347 The Cauchy–Schwarz inequality and the definition of the energy norm (2.2) lead to

$$\left\| \nabla(w_1 - w_2) \right\| \leq \sum_{\alpha=1}^2 \beta_\alpha^{-\frac{1}{2}} \left\| \beta_\alpha^{\frac{1}{2}} \nabla w_\alpha \right\| \leq \left( \sum_{\alpha=1}^2 \beta_\alpha^{-1} \right)^{\frac{1}{2}} \left( \sum_{\alpha=1}^2 \left\| \beta_\alpha^{\frac{1}{2}} \nabla w_\alpha \right\|^2 \right)^{\frac{1}{2}} \leq \left( \frac{1}{\beta_1} + \frac{1}{\beta_2} \right)^{\frac{1}{2}} \left\| \mathbf{w} \right\|. \tag{7.12}$$

348 The Poincaré–Friedrichs inequality (2.1a) together with (7.12) give

$$-b(\mathbf{w}, \lambda_h^{j,k,i}) \leq \eta_{\text{sm,lin,alg},1}^{j,k,i} \left\| \mathbf{u} - \tilde{\mathbf{s}}_h^{j,k,i} \right\| + \frac{1}{2} \sum_{K \in \mathcal{T}_h} \underbrace{2 \left( \lambda_h^{j,k,i,\text{pos}}, \tilde{\mathbf{s}}_{1h}^{j,k,i} - \tilde{\mathbf{s}}_{2h}^{j,k,i} \right)}_{\eta_{\text{sm,lin,alg},2,K}^{j,k,i}}. \quad (7.13)$$

349 Finally, due to the results (7.8), (7.9), (7.10), and (7.13) we have

$$\left\| \mathbf{u} - \tilde{\mathbf{s}}_h^{j,k,i} \right\|^2 \leq \left( \eta_{\text{osc}} + \eta_{\text{alg}}^{j,k,i} + \eta_{\text{monc}}^{j,k,i} + \eta_{\text{sm,lin,alg},1}^{j,k,i} \right) \left\| \mathbf{u} - \tilde{\mathbf{s}}_h^{j,k,i} \right\| + \frac{1}{2} \sum_{K \in \mathcal{T}_h} \eta_{\text{sm,lin,alg},2,K}^{j,k,i}. \quad (7.14)$$

350 The Young inequality  $ab \leq \frac{1}{2}(a^2 + b^2)$ ,  $(a, b) \geq 0$ , applied to the first term of (7.14) finally gives

$$\left\| \mathbf{u} - \tilde{\mathbf{s}}_h^{j,k,i} \right\| \leq \eta^{j,k,i} := \left\{ \left( \eta_{\text{osc}} + \eta_{\text{alg}}^{j,k,i} + \eta_{\text{monc}}^{j,k,i} + \eta_{\text{sm,lin,alg},1}^{j,k,i} \right)^2 + \sum_{K \in \mathcal{T}_h} \eta_{\text{sm,lin,alg},2,K}^{j,k,i} \right\}^{\frac{1}{2}}.$$

351 **Case 2.** If  $\left\| \mathbf{u} - \tilde{\mathbf{s}}_h^{j,k,i} \right\| \leq \left\| \mathbf{u} - \tilde{\mathbf{u}}_h^{j,k,i} \right\|$ , we have

$$\left\| \mathbf{u} - \tilde{\mathbf{u}}_h^{j,k,i} \right\|^2 = a(\mathbf{u} - \tilde{\mathbf{u}}_h^{j,k,i}, \mathbf{u} - \tilde{\mathbf{u}}_h^{j,k,i}) = a(\mathbf{u} - \tilde{\mathbf{u}}_h^{j,k,i}, \mathbf{u} - \tilde{\mathbf{s}}_h^{j,k,i}) + a(\mathbf{u} - \tilde{\mathbf{u}}_h^{j,k,i}, \tilde{\mathbf{s}}_h^{j,k,i} - \tilde{\mathbf{u}}_h^{j,k,i}). \quad (7.15)$$

352 We start by estimating the first term of (7.15), while still denoting  $\mathbf{w} = \mathbf{u} - \tilde{\mathbf{s}}_h^{j,k,i}$ , as

$$\begin{aligned} a(\mathbf{u} - \tilde{\mathbf{u}}_h^{j,k,i}, \mathbf{w}) &\leq l(\mathbf{w}) - a(\tilde{\mathbf{u}}_h^{j,k,i}, \mathbf{w}) + b(\mathbf{w}, \lambda_h^{j,k,i}) - b(\mathbf{w}, \lambda_h^{j,k,i}) \\ &\leq \sum_{\alpha=1}^2 \left( f_\alpha - (-1)^\alpha \lambda_h^{j,k,i}, w_\alpha \right) - \sum_{\alpha=1}^2 \beta_\alpha \left( \nabla \tilde{u}_{\alpha h}^{j,k,i}, \nabla w_\alpha \right) - b(\mathbf{w}, \lambda_h^{j,k,i}), \end{aligned} \quad (7.16)$$

353 using again (2.4) and (2.8), as in (7.5). The three terms in (7.16) are identical to the terms in (7.5), estimated  
354 in (7.8), (7.9), and (7.13), respectively. Invoking the hypothesis of this case, we can thus write

$$\begin{aligned} a(\mathbf{u} - \tilde{\mathbf{u}}_h^{j,k,i}, \mathbf{w}) &\leq \left( \eta_{\text{osc}} + \eta_{\text{alg}}^{j,k,i} + \eta_{\text{sm,lin,alg},1}^{j,k,i} \right) \left\| \mathbf{u} - \tilde{\mathbf{s}}_h^{j,k,i} \right\| + \frac{1}{2} \sum_{K \in \mathcal{T}_h} \eta_{\text{sm,lin,alg},2,K}^{j,k,i} \\ &\leq \left( \eta_{\text{osc}} + \eta_{\text{alg}}^{j,k,i} + \eta_{\text{sm,lin,alg},1}^{j,k,i} \right) \left\| \mathbf{u} - \tilde{\mathbf{u}}_h^{j,k,i} \right\| + \frac{1}{2} \sum_{K \in \mathcal{T}_h} \eta_{\text{sm,lin,alg},2,K}^{j,k,i}. \end{aligned}$$

355 The Cauchy–Schwarz inequality yields for the second term of (7.15)

$$a(\mathbf{u} - \tilde{\mathbf{u}}_h^{j,k,i}, \tilde{\mathbf{s}}_h^{j,k,i} - \tilde{\mathbf{u}}_h^{j,k,i}) \leq \left\| \tilde{\mathbf{s}}_h^{j,k,i} - \tilde{\mathbf{u}}_h^{j,k,i} \right\| \left\| \mathbf{u} - \tilde{\mathbf{u}}_h^{j,k,i} \right\| = \eta_{\text{monc}}^{j,k,i} \left\| \mathbf{u} - \tilde{\mathbf{u}}_h^{j,k,i} \right\|.$$

356 By combining the previous results, we then obtain

$$\left\| \mathbf{u} - \tilde{\mathbf{u}}_h^{j,k,i} \right\|^2 \leq \left( \eta_{\text{osc}} + \eta_{\text{alg}}^{j,k,i} + \eta_{\text{monc}}^{j,k,i} + \eta_{\text{sm,lin,alg},1}^{j,k,i} \right) \left\| \mathbf{u} - \tilde{\mathbf{u}}_h^{j,k,i} \right\| + \frac{1}{2} \sum_{K \in \mathcal{T}_h} \eta_{\text{sm,lin,alg},2,K}^{j,k,i}. \quad (7.17)$$

357 The Young inequality  $ab \leq \frac{1}{2}(a^2 + b^2)$ ,  $(a, b) \geq 0$ , applied to the first term of (7.17) provides now again  
358 immediately the desired result.  $\square$

## 359 7.2 A posteriori error estimate for the actions

360 We present here an a posteriori estimate for the actions  $\lambda_h^{j,k,i}$ , extending [7, Corollary 3.5] to the nonconforming  
361 and inexact solvers setting.

362 **Theorem 7.3** (A posteriori estimate for the actions). *Let the assumptions and notations of Theorem 7.1*  
363 *hold. The following a posteriori error estimate holds between the solution  $\lambda \in \Lambda$  of problem (2.6) and the*

364 approximation  $\lambda_h^{j,k,i}$  given by (4.7)–(4.8)

$$\left\| \lambda - \lambda_h^{j,k,i} \right\|_{H_*^{-1}(\Omega)} \leq \eta_{\text{osc}} + \eta_{\text{alg}}^{j,k,i} + \eta^{j,k,i}. \quad (7.18)$$

365 *Proof.* Let  $\beta_m := \max(\beta_1, \beta_2)$ . From the definition (2.3) of the norm of  $H_*^{-1}(\Omega)$  and of the form  $b$  in (2.4) we  
366 have

$$\left\| \lambda - \lambda_h^{j,k,i} \right\|_{H_*^{-1}(\Omega)} = \sup_{\substack{v \in H_0^1(\Omega) \\ \beta_m \|\nabla v\|^2 = 1}} (\lambda - \lambda_h^{j,k,i}, v) = \sup_{\substack{\varphi \in [H_0^1(\Omega)]^2 \\ \beta_m \sum_{\alpha=1}^2 \|\nabla \varphi_\alpha\|^2 = 1}} b(\varphi, \lambda - \lambda_h^{j,k,i}).$$

367 Fix  $\varphi \in [H_0^1(\Omega)]^2$  such that  $\beta_m \sum_{\alpha=1}^2 \|\nabla \varphi_\alpha\|^2 = 1$ . It follows from (2.6a) that  $-b(\varphi, \lambda - \lambda_h^{j,k,i}) = l(\varphi) -$   
368  $a(\mathbf{u}, \varphi) + b(\varphi, \lambda_h^{j,k,i})$ . By simply adding and subtracting  $a(\tilde{\mathbf{u}}_h^{j,k,i}, \varphi)$ , where the action of the form  $a$  on  $\tilde{\mathbf{u}}_h^{j,k,i}$  is  
369 defined in (2.5), we obtain

$$-b(\varphi, \lambda - \lambda_h^{j,k,i}) = l(\varphi) + b(\varphi, \lambda_h^{j,k,i}) - a(\tilde{\mathbf{u}}_h^{j,k,i}, \varphi) - a(\mathbf{u} - \tilde{\mathbf{u}}_h^{j,k,i}, \varphi).$$

The first three terms are identical to the first three terms in (7.5) but with  $\varphi$  instead of  $\mathbf{w}$ . They are estimated  
in (7.8) and (7.9), leading to

$$l(\varphi) + b(\varphi, \lambda_h^{j,k,i}) - a(\tilde{\mathbf{u}}_h^{j,k,i}, \varphi) \leq (\eta_{\text{osc}} + \eta_{\text{alg}}^{j,k,i}) \|\varphi\|.$$

370 The last term is estimated as  $-a(\mathbf{u} - \tilde{\mathbf{u}}_h^{j,k,i}, \varphi) \leq \left\| \mathbf{u} - \tilde{\mathbf{u}}_h^{j,k,i} \right\|$ , since  $\|\varphi\| \leq 1$ . Through these estimations  
371 we get

$$-b(\varphi, \lambda - \lambda_h^{j,k,i}) \leq \eta_{\text{osc}} + \eta_{\text{alg}}^{j,k,i} + \left\| \mathbf{u} - \tilde{\mathbf{u}}_h^{j,k,i} \right\|. \quad (7.19)$$

372 We obtain the desired result by combining (7.19) to (7.3a).  $\square$

### 373 7.3 Distinguishing the different error components

374 The aim of this section is to identify the various error components in the a posteriori estimators from Theorem  
375 7.1, which will lead to a posteriori stopping criteria.

376 **Corollary 7.4** (A posteriori error estimate distinguishing the error components). *We define for  $\alpha \in \{1, 2\}$  and*  
377  *$K \in \mathcal{T}_h$  the smoothing, discretization, linearization, and algebraic estimators as follows:*

$$\eta_{\text{disc}}^{j,k,i} := \eta_{\text{osc}} + \eta_{\text{nonc}}^{j,k,i} + \left( \sum_{K \in \mathcal{T}_h} 2 \left( \lambda_h^{j,k,i,\text{pos}}, \tilde{s}_{1h}^{j,k,i} - \tilde{s}_{2h}^{j,k,i} - \tilde{u}_{1h}^{j,k,i} + \tilde{u}_{2h}^{j,k,i} \right)_K \right)^{\frac{1}{2}}, \quad (7.20a)$$

$$\eta_{\text{sm,lin,alg}}^{j,k,i} := \eta_{\text{sm,lin,alg,1}}^{j,k,i} + \left( \sum_{K \in \mathcal{T}_h} 2 \left( \lambda_h^{j,k,i,\text{pos}}, u_{1h}^{j,k,i} - u_{2h}^{j,k,i} \right)_K \right)^{\frac{1}{2}}, \quad (7.20b)$$

$$\eta_{\text{lin,alg}}^{j,k,i} := \eta_{\text{lin,alg,1}}^{j,k,i} + \left( \sum_{K \in \mathcal{T}_h} 2 \left( \lambda_h^{j,k,i,\text{pos}} - \lambda_h^{j,k-1,\bar{i},\text{pos}}, u_{1h}^{j,k,i} - u_{2h}^{j,k,i} - u_{1h}^{j,k-1,\bar{i}} + u_{2h}^{j,k-1,\bar{i}} \right)_K \right)^{\frac{1}{2}}, \quad (7.20c)$$

$$\eta_{\text{alg}}^{j,k,i} := \left( \sum_{K \in \mathcal{T}_h} \sum_{\alpha=1}^2 \left( \eta_{\text{alg},K,\alpha}^{j,k,i} \right)^2 \right)^{\frac{1}{2}}, \quad (7.20d)$$

378 with

$$\eta_{\text{lin,alg,1,K}}^{j,k,i} := C_{\beta,\Omega} \left\| \lambda_h^{j,k,i,\text{neg}} - \lambda_h^{j,k-1,\bar{i},\text{neg}} \right\|_K, \quad \text{and} \quad \eta_{\text{lin,alg,1}}^{j,k,i} := \left( \sum_{K \in \mathcal{T}_h} \left( \eta_{\text{lin,alg,1,K}}^{j,k,i} \right)^2 \right)^{\frac{1}{2}}.$$

379 Then,

$$\left\| \mathbf{u} - \tilde{\mathbf{u}}_h^{j,k,i} \right\| \leq \eta^{j,k,i} \leq \eta_{\text{disc}}^{j,k,i} + \eta_{\text{sm,lin,alg}}^{j,k,i} + \eta_{\text{lin,alg}}^{j,k,i} + \eta_{\text{alg}}^{j,k,i}. \quad (7.21)$$

380 *Proof.* From (7.3a), employing the inequality  $(a+b)^{\frac{1}{2}} \leq a^{\frac{1}{2}} + b^{\frac{1}{2}}$ , for  $a, b \geq 0$ , we have

$$\left\| \mathbf{u} - \tilde{\mathbf{u}}_h^{j,k,i} \right\| \leq \eta^{j,k,i} \leq \eta_{\text{osc}} + \eta_{\text{alg}}^{j,k,i} + \eta_{\text{nonc}}^{j,k,i} + \eta_{\text{sm,lin,alg,1}}^{j,k,i} + \left( \sum_{K \in \mathcal{T}_h} \eta_{\text{sm,lin,alg,2,K}}^{j,k,i} \right)^{\frac{1}{2}}. \quad (7.22)$$

381 We then decompose  $\eta_{\text{sm,lin,alg},2,K}^{j,k,i}$  by adding and subtracting the components of  $\tilde{\mathbf{u}}_h^{j,k,i}$  as follows

$$\begin{aligned}
\eta_{\text{sm,lin,alg},2,K}^{j,k,i} &= 2 \left( \lambda_h^{j,k,i,\text{pos}}, \tilde{s}_{1h}^{j,k,i} - \tilde{s}_{2h}^{j,k,i} \right)_K \\
&= 2 \left( \lambda_h^{j,k,i,\text{pos}}, \tilde{s}_{1h}^{j,k,i} - \tilde{s}_{2h}^{j,k,i} - \tilde{u}_{1h}^{j,k,i} + \tilde{u}_{2h}^{j,k,i} \right)_K + 2 \left( \lambda_h^{j,k,i,\text{pos}}, \tilde{u}_{1h}^{j,k,i} - \tilde{u}_{2h}^{j,k,i} \right)_K \\
&\stackrel{(5.1a)}{=} 2 \left( \lambda_h^{j,k,i,\text{pos}}, \tilde{s}_{1h}^{j,k,i} - \tilde{s}_{2h}^{j,k,i} - \tilde{u}_{1h}^{j,k,i} + \tilde{u}_{2h}^{j,k,i} \right)_K + 2 \left( \lambda_h^{j,k,i,\text{pos}}, u_{1h}^{j,k,i} - u_{2h}^{j,k,i} \right)_K.
\end{aligned} \tag{7.23}$$

We now combine (7.23) together with (7.22) inserting the absolute values. This leads to

$$\left\| \mathbf{u} - \tilde{\mathbf{u}}_h^{j,k,i} \right\| \leq \eta_{\text{disc}}^{j,k,i} + \eta_{\text{sm,lin,alg}}^{j,k,i} + \eta_{\text{alg}}^{j,k,i}.$$

382 Finally, we define the linearization estimator  $\eta_{\text{lin,alg}}^{j,k,i}$  analogously to the smoothing estimator  $\eta_{\text{sm,lin,alg}}^{j,k,i}$ , consid-  
383 ering the terms  $\lambda_h^{j,k,i} - \lambda_h^{j,k-1,\bar{i}}$  and  $\mathbf{u}_h^{j,k,i} - \mathbf{u}_h^{j,k-1,\bar{i}}$  estimating the linearization error.  $\square$

384 **Remark 7.5** (Nature of the estimators). *The nonconformity and oscillation estimators  $\eta_{\text{nonc}}^{j,k,i}$  and  $\eta_{\text{osc}}$  considered  
385 as discretization estimators vanish when the computational effort grows, i.e. when the number of mesh elements  
386 goes to infinity. The smoothing estimator  $\eta_{\text{sm,lin,alg}}^{j,k,i}$  stems from the error in the algebraic system, linearization,  
387 and smoothing. It goes to zero at convergence of all the solvers, since when  $j, k$ , and  $i \rightarrow \infty$ , we have  $\lambda_h^{j,k,i} \geq$   
388 0 and  $\lambda_h^{j,k,i} (u_{1h}^{j,k,i} - u_{2h}^{j,k,i}) = 0$ . The linearization estimator  $\eta_{\text{lin,alg}}^{j,k,i}$  reflects the error stemming from both  
389 linearization and algebraic resolution and vanishes when  $j$  and  $i \rightarrow \infty$ . Finally, the algebraic estimator  $\eta_{\text{alg}}^{j,k,i}$   
390 evaluating the error in the algebraic iterative resolution of the linear system (4.4) vanishes when  $i \rightarrow \infty$ .*

## 391 8 Stopping criteria and adaptive inexact smoothing algorithm

392 We derive in this section adaptive stopping criteria for the linear, the nonlinear solver, and the smoothing  
393 iterations, based on the estimators of Corollary 7.4.

394 Let three user-specified parameters  $\zeta_{\text{sm}}$ ,  $\zeta_{\text{lin}}$ , and  $\zeta_{\text{alg}}$  be given in  $]0, 1]$ , representing the desired relative size  
395 (percentage) of the smoothing, linearization, and algebraic errors, respectively. Below, we denote by  $\bar{j}, \bar{k}$ , and  
396  $\bar{i}$  the last (stopping) smoothing, linearization and algebraic step, respectively. The stopping criterion for the  
397 algebraic step  $i$  at each linearization step  $k$  and smoothing step  $j$  is chosen as

$$\eta_{\text{alg}}^{j,k,\bar{i}} < \zeta_{\text{alg}} \eta_{\text{lin,alg}}^{j,k,\bar{i}}. \tag{8.1}$$

398 This criterion expresses that there is no need to continue with the algebraic iterations once the linearization  
399 error component starts to dominate. Similarly, to stop the Newton iterations at each smoothing step  $j$ , we  
400 apply

$$\eta_{\text{lin,alg}}^{j,\bar{k},\bar{i}} < \zeta_{\text{lin}} \eta_{\text{disc}}^{j,\bar{k},\bar{i}}, \tag{8.2}$$

401 which requires the linearization estimator to be sufficiently small with respect to the discretization estimator.  
402 Finally, we stop the outer smoothing loop whenever

$$\eta_{\text{sm,lin,alg}}^{\bar{j},\bar{k},\bar{i}} < \zeta_{\text{sm}} \eta_{\text{disc}}^{\bar{j},\bar{k},\bar{i}}, \tag{8.3}$$

403 i.e. when the smoothing estimator is  $\zeta_{\text{sm}}$ -times smaller than the discretization estimator. As for the amount of  
404 smoothing, we will proceed following [8] and diminish it by a fixed factor  $\zeta \in ]0, 1[$  on each smoothing step. We  
405 are now ready to present our adaptive inexact smoothing Newton algorithm that includes the above adaptive  
406 criteria for stopping the iterative solvers.

---

**Algorithm 1** Adaptive inexact smoothing Newton algorithm
 

---

**1. Initialization**

Choose parameters  $\zeta \in ]0, 1[$  and  $\zeta_{\text{sm}}, \zeta_{\text{lin}}, \zeta_{\text{alg}} \in ]0, 1]$ .

Choose an initial smoothing parameter  $\mu^1 > 0$ , a number of additional algebraic solver steps  $\nu \geq 1$ , and an initial approximation  $\mathbf{X}^0 \in \mathbb{R}^n$ . Set  $j := 1$  and  $\bar{j} = 0$ .

**2. Smoothing  $j$ -loop**

**2.1** Set  $\mathbf{X}^{j,0} := \mathbf{X}^0$ ,  $k := 1$ , and  $\bar{k} = 0$ .

**2.2 Newton linearization  $k$ -loop**

**2.2.1** From  $\mathbf{X}^{j,k-1}$  define  $\mathbb{A}_{\mu^j}^{j,k-1} \in \mathbb{R}^{n,n}$  and  $\mathbf{B}_{\mu^j}^{j,k-1} \in \mathbb{R}^n$  by the Newton linearization (4.5).

**2.2.2** Consider the problem of finding a solution  $\mathbf{X}^{j,k}$  to

$$\mathbb{A}_{\mu^j}^{j,k-1} \mathbf{X}^{j,k} = \mathbf{B}_{\mu^j}^{j,k-1}. \quad (8.4)$$

**2.2.3** Set  $\mathbf{X}^{j,k,0} := \mathbf{X}^{j,k-1}$  as initial guess for the iterative algebraic solver.

Set  $i := 1$ , and if  $j = 1$  and  $k = 1$ , set  $\bar{i} = 0$ .

**2.2.4 Algebraic solver  $i$ -loop**

i) Perform  $\nu$  steps of the iterative algebraic solver for the solution of (8.4), yielding, on step  $i + \nu$ , an approximation  $\mathbf{X}^{j,k,i+\nu}$  to  $\mathbf{X}^{j,k}$  satisfying

$$\mathbb{A}_{\mu^j}^{j,k-1} \mathbf{X}^{j,k,i+\nu} = \mathbf{B}_{\mu^j}^{j,k-1} - \mathbf{R}_{\text{alg}}^{j,k,i+\nu}.$$

ii) Set  $i := i + \nu$ . Compute the estimators given in (7.20).

iii) If  $\eta_{\text{alg}}^{j,k,i} < \zeta_{\text{alg}} \eta_{\text{lin,alg}}^{j,k,i}$ , set  $\bar{i} := i$  and stop. If not, go to i).

**2.2.5** If  $\eta_{\text{lin,alg}}^{j,k,\bar{i}} < \zeta_{\text{lin}} \eta_{\text{disc}}^{j,k,\bar{i}}$ , set  $\bar{k} := k$  and stop. If not, set  $k := k + 1$  and go to **2.2.1**.

**2.3** If  $\eta_{\text{sm,lin,alg}}^{j,\bar{k},\bar{i}} < \zeta_{\text{sm}} \eta_{\text{disc}}^{j,\bar{k},\bar{i}}$ , set  $\bar{j} := j$  and stop.

If not, set  $j := j + 1$ ,  $\mathbf{X}^{j,0} := \mathbf{X}^{j-1,\bar{k},\bar{i}}$ , and  $\mu^j := \zeta \mu^{j-1}$ . Then set  $k := 1$  and go to **2.2.1**.

---

## 9 Numerical results

407

In this section, we numerically illustrate the efficiency of our theoretical developments considering problem (1.6). Our main goals are to assess the sharpness of the guaranteed bound (7.3) and to show that Algorithm 1 performs well and leads to smaller number of iterations in comparison with usual stopping criteria as well as the classical semismooth Newton method.

We carry out computations fixing the tensions in (1.6a) and (1.6b) as  $\beta_1 = 1$  and  $\beta_2 = 1$ . The boundary condition  $g$  of the first membrane in (1.6d) is taken equal to 0.1. We consider the one-dimensional domain  $\Omega = (-1, 1)$ , (all the theoretical developments apply here), and use the following analytical solution for  $x \in \Omega$ , following [7],

$$u_1(x) := g(2x^2 - 1), \quad u_2(x) := \begin{cases} 2g(1 - x^2)(2x^2 - 1) & \text{if } x < \frac{-1}{\sqrt{2}} \text{ or } x > \frac{1}{\sqrt{2}}, \\ g(2x^2 - 1) & \text{otherwise,} \end{cases} \quad \lambda(x) := \begin{cases} 0 & \text{if } x < \frac{-1}{\sqrt{2}} \text{ or } x > \frac{1}{\sqrt{2}}, \\ 2g & \text{otherwise.} \end{cases}$$

This triple is the solution of (1.6) for the data  $f_1$  and  $f_2$  given by

$$f_1(x) := \begin{cases} -4g & \text{if } x < \frac{-1}{\sqrt{2}} \text{ or } x > \frac{1}{\sqrt{2}}, \\ -6g & \text{otherwise,} \end{cases} \quad f_2(x) := \begin{cases} -12g(1 - 4x^2) & \text{if } x < \frac{-1}{\sqrt{2}} \text{ or } x > \frac{1}{\sqrt{2}}, \\ -2g & \text{otherwise.} \end{cases}$$

For all the tests, the number of mesh elements is  $m = 10000$ , leading to the overall number of unknowns  $n = 30000$ . We choose the initial guess as  $\mathbf{X}^0 = [\mathbf{1}g, \mathbf{0}, \mathbf{0}] \in \mathbb{R}^n$ , where  $\mathbf{1} = [1, \dots, 1]^T \in \mathbb{R}^m$ . The implementation was done in the MATLAB software. The value of the coefficients  $\zeta_{\text{sm}}, \zeta_{\text{lin}}$ , and  $\zeta_{\text{alg}}$  from the adaptive stopping criteria in Section 8 is 0.1. The parameters in Algorithm 1 are set as:  $\mu^1 = 1$ ,  $\zeta = 0.1$ , and  $\nu = 4$ .

420

## 421 9.1 Semismooth Newton-min

422 First, for comparison, to find an approximate solution to the algebraic system (2.11), we employ the semismooth  
 423 Newton-min method described in Section 3 in which the stopping criterion for the linearization requests the  
 424 relative total residual of problem (3.3)  $\mathbf{R}_{\text{rel}}^k := \|\mathbf{R}(\mathbf{X}^k)\|/\|\mathbf{R}(\mathbf{X}^0)\|$  to be below  $10^{-8}$ , where

$$\mathbf{R}(\mathbf{V}) := \begin{bmatrix} \mathbf{F} - \mathbb{E}\mathbf{V} \\ -\mathbf{C}(\mathbf{V}) \end{bmatrix}, \quad \mathbf{V} \in \mathbb{R}^n. \quad (9.1)$$

425 The evolution of the relative total residual is shown in Figure 6. In its right part, we zoom on the last 10  
 426 Newton-min iterations. We observe that the curve goes down slowly until step 893, where the convergence gets  
 427 extremely fast.

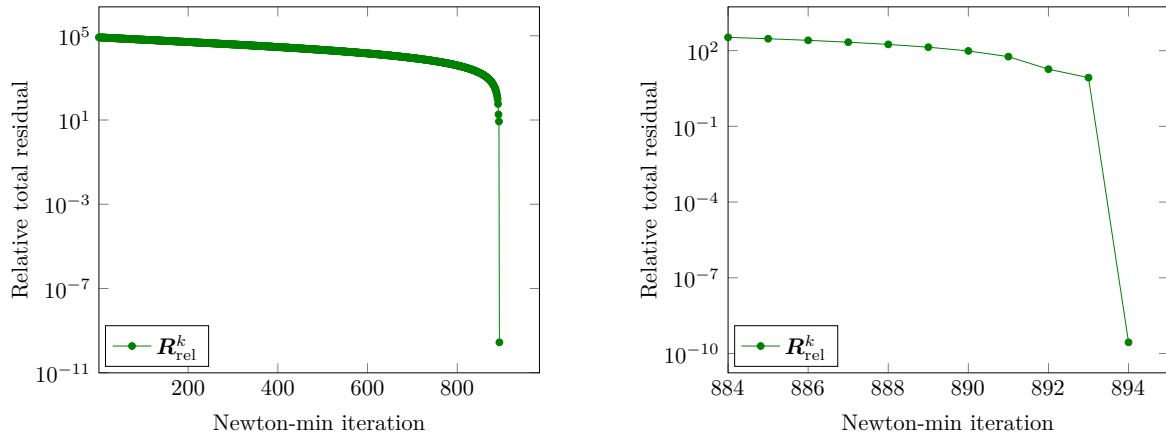


Figure 6: [Semismooth Newton-min method of Section 3] Relative total residual as a function of Newton-min iterations, left, and as a function of the last 10 Newton-min iterations, right.

## 428 9.2 Adaptive smoothing Newton-min

429 In this section, we employ Algorithm 1 with an “exact” resolution of the system of algebraic equations (8.4),  
 430 i.e., we skip steps 2.2.3 and 2.2.4. We drop the notation “alg” from estimators (7.20b) and (7.20c), whereas  
 431  $\eta_{\text{alg}}^{j,k,i}$  of (7.20d) vanishes. First, we want to emphasize the performance of the adaptive smoothing method  
 432 employing the adaptive stopping criterion to stop the nonlinear solver. To this end, we use two linearization  
 433 stopping criteria: the adaptive criterion (8.2)  $\eta_{\text{lin}}^{j,k} < \zeta_{\text{lin}}\eta_{\text{disc}}^{j,k}$  and the classical one on the relative linearization  
 434 residual of problem (4.3)  $\mathbf{R}_{\text{lin,rel}}^{j,k} := \|\mathbf{R}_{\text{lin}}(\mathbf{X}^{j,k})\|/\|\mathbf{R}_{\text{lin}}(\mathbf{X}^{1,0})\|$  lying below  $10^{-8}$ , with  $\mathbf{R}_{\text{lin}}(\cdot)$  given by

$$\mathbf{R}_{\text{lin}}(\mathbf{V}) := \begin{bmatrix} \mathbf{F} - \mathbb{E}\mathbf{V} \\ -\mathbf{C}_{\mu^j}(\mathbf{V}) \end{bmatrix}, \quad \mathbf{V} \in \mathbb{R}^n. \quad (9.2)$$

435 We show in Figure 7 the number of performed Newton iterations employing the smoothing Newton method  
 436 with exact algebraic resolution, during the fourth smoothing step ( $j = 4$ ). It can be noticed that the use of the  
 437 adaptive stopping criterion brings down the number of iterations from 20 to 12.

438 We now employ the adaptive smoothing Newton-min method, with an exact algebraic resolution, including  
 439 the adaptive stopping criteria (8.2) and (8.3) to stop the linearization and smoothing steps, respectively. In  
 440 terms of numbers, 6 smoothing iterations and 52 cumulated linearization iterations are needed to reach the end  
 441 of the simulation, as seen from Figure 8 left, compared to 894 linearization iterations employing the semismooth  
 442 Newton-min method above.

443 The various estimators given in (7.20) are presented in the left part of Figure 8. Each set of curves represents  
 444 one smoothing step (fixed value  $j$ ). From each set one can see that the linearization estimator is dominant and  
 445 close to the total estimator, until becoming smaller than the discretization estimator, when the adaptive stopping  
 446 criterion  $\eta_{\text{lin}}^{j,k} < \zeta_{\text{lin}}\eta_{\text{disc}}^{j,k}$  is satisfied. The smoothing estimator satisfies (8.3) from the cumulated Newton-min  
 447 iteration  $k = 51$ . Computational savings in terms of linearization iterations can be evaluated considering  
 448 the results in Figure 8, right. A comparison of the number of performed Newton iterations employing the  
 449 semismooth Newton-min method of Section 9.1 and the adaptive smoothing Newton-min method of the present  
 450 section shows a significant gain reaching a factor of roughly 17.

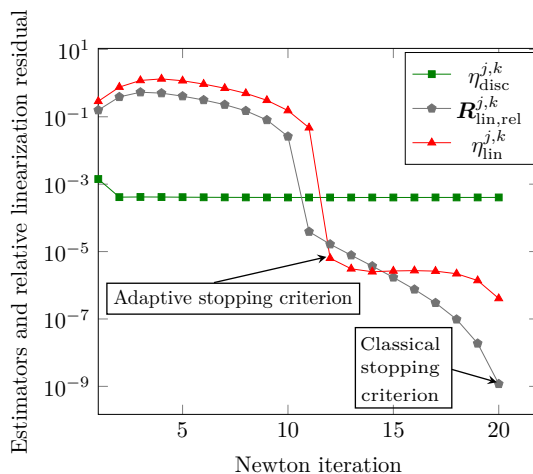


Figure 7: [Adaptive smoothing Newton-min method, Algorithm 1, exact resolution of the algebraic system (8.4)] Estimators and relative linearization residual as a function of the Newton iterations at a specific smoothing step ( $j = 4$ ,  $k$  varies).

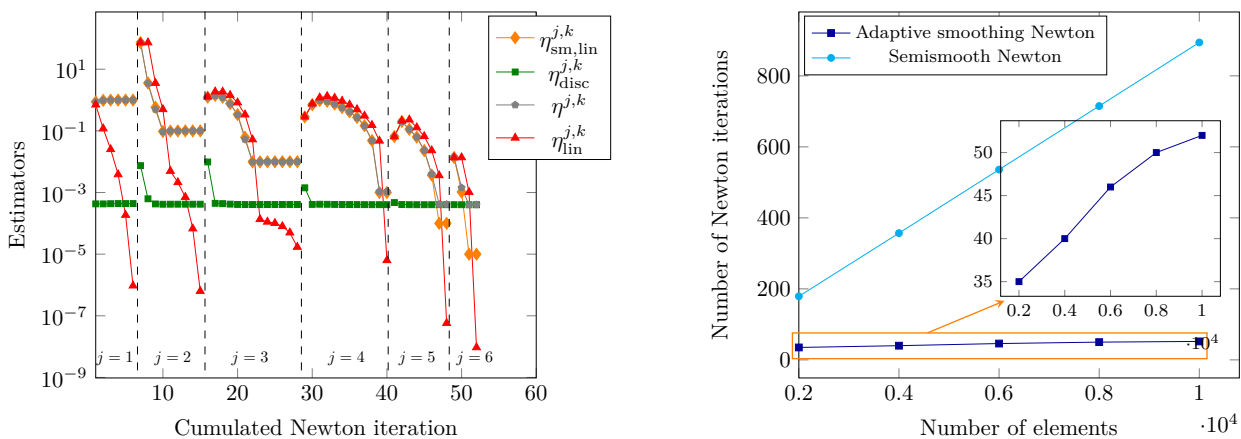


Figure 8: [Adaptive smoothing Newton-min method, Algorithm 1, exact resolution of the algebraic system (8.4)] Estimators as a function of the cumulated Newton iterations, left. Comparison between the number of performed Newton iterations employing the Newton-min method of Section 9.1 and the adaptive smoothing Newton-min method of Section 9.2, right.

### 9.3 Adaptive inexact smoothing Newton-min

This section is devoted to present the results obtained employing the adaptive inexact smoothing Newton-min algorithm of Algorithm 1 in Section 8. We consider at each Newton step  $k \geq 1$  the GMRES iterative algebraic solver for the system (8.4), see [50], with an ILU preconditioner. To shed more light on the importance of the adaptive stopping criterion for stopping the linear solver, we compare the adaptive resolution where the stopping criterion for the GMRES is given by (8.1) with the classical resolution where the algebraic iterations are stopped using the relative algebraic residual, i.e.,

$$\mathbf{R}_{\text{alg,rel}}^{j,k,i} := \frac{\|\mathbb{M}_2 \setminus (\mathbb{M}_1 \setminus (\mathbf{B}_{\mu^j}^{j,k-1} - \mathbb{A}_{\mu^j}^{j,k-1} \mathbf{X}^{j,k,i}))\|}{\|\mathbb{M}_2 \setminus (\mathbb{M}_1 \setminus (\mathbf{B}_{\mu^j}^{j,k-1} - \mathbb{A}_{\mu^j}^{j,k-1} \mathbf{X}^{j,k-1}))\|} \leq 10^{-10}, \quad (9.3)$$

where  $\mathbb{M}_1$  and  $\mathbb{M}_2$  denote the preconditioner matrices. Figure 9 shows the algebraic estimator, linearization estimator, and relative algebraic residual, computed every  $\nu = 4$  algebraic steps, at specific smoothing and linearization steps  $(j, k) = (3, 7)$  for the classical and adaptive resolutions. We observe that only 12 algebraic iterations are required to satisfy (8.1), whereas 64 iterations are needed to meet the classical criterion (9.3).

We now employ the entire Algorithm 1 featuring also the adaptive stopping criterion for the algebraic solver. To satisfy adaptive criteria (8.1), (8.2), and (8.3), 6 smoothing iterations, 55 cumulated Newton-min iterations, and 3020 cumulated GMRES iterations are needed. We also assess the quality of the a posteriori error estimates of Theorems 7.1 and 7.3 by means of the effectivity indices resulting from estimates (7.3a), (7.3b), and (7.18)

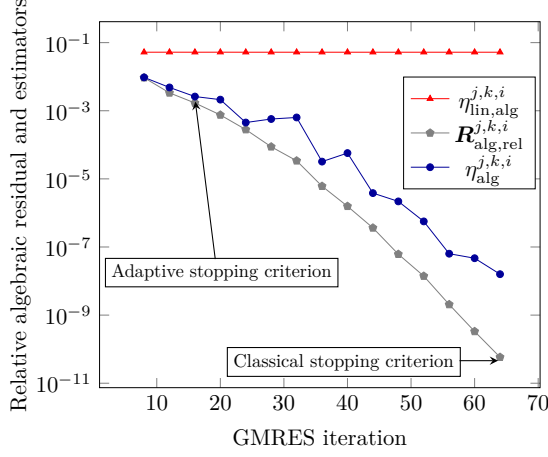


Figure 9: [Adaptive inexact smoothing Newton-min method, Algorithm 1] Estimators and relative algebraic residual as a function of the GMRES iterations at smoothing and linearization steps  $(j, k) = (3, 7)$  using the adaptive stopping criterion (8.1) and the classical one (9.3).

466 defined as

$$\mathbb{I}_{\text{eff}}^{j,k,i} := \frac{\eta^{j,k,i}}{\|\mathbf{u} - \tilde{\mathbf{u}}_h^{j,k,i}\|}, \quad (9.4a)$$

$$\bar{\mathbb{I}}_{\text{eff}}^{j,k,i} := \frac{\eta^{j,k,i} + \left\{ \sum_{\sigma \in \mathcal{E}_h} |\sigma|^{-1} \|\Pi_0^\sigma(\tilde{\mathbf{u}}_h^{j,k,i})\|_\sigma^2 \right\}^{\frac{1}{2}}}{\|\mathbf{u} - \tilde{\mathbf{u}}_h^{j,k,i}\| + \left\{ \sum_{\sigma \in \mathcal{E}_h} |\sigma|^{-1} \|\mathbf{u} - \Pi_0^\sigma(\tilde{\mathbf{u}}_h^{j,k,i})\|_\sigma^2 \right\}^{\frac{1}{2}}}, \quad (9.4b)$$

$$\tilde{\mathbb{I}}_{\text{eff}}^{j,k,i} := \frac{\eta_{\text{osc}} + \eta_{\text{alg}}^{j,k,i} + 2\eta^{j,k,i} + \left\{ \sum_{\sigma \in \mathcal{E}_h} |\sigma|^{-1} \|\mathbf{u} - \Pi_0^\sigma(\tilde{\mathbf{u}}_h^{j,k,i})\|_\sigma^2 \right\}^{\frac{1}{2}}}{\|\mathbf{u} - \tilde{\mathbf{u}}_h^{j,k,i}\| + \|\lambda - \lambda_h^{j,k,i}\|_{H_*^{-1}(\Omega)} + \left\{ \sum_{\sigma \in \mathcal{E}_h} |\sigma|^{-1} \|\mathbf{u} - \Pi_0^\sigma(\tilde{\mathbf{u}}_h^{j,k,i})\|_\sigma^2 \right\}^{\frac{1}{2}}}. \quad (9.4c)$$

467 See Remark 9.1 for details on approximately computing the dual norm.

468 **Remark 9.1** (Computing approximately the dual norm). *In practice, the dual norm  $\|\lambda - \lambda_h^{j,k,i}\|_{H^{-1}(\Omega)}$  with*  
 469  *$\lambda - \lambda_h^{j,k,i} \in \Lambda$ , is not easily computable. We provide here a practical way to approximate this norm and evaluate*  
 470 *it numerically following [21]. We consider the following elliptic problem that consists in finding, for a given*  
 471  *$f \in L^2(\Omega)$ , the function  $\phi : \Omega \rightarrow \mathbb{R}$  such that*

$$\begin{aligned} -\Delta\phi &= f && \text{in } \Omega, \\ \phi &= 0 && \text{on } \partial\Omega. \end{aligned} \quad (9.5)$$

472 The weak formulation of problem (9.5) consists in finding  $\phi \in H_0^1(\Omega)$  such that

$$(\nabla\phi, \nabla v) = (f, v) \quad \forall v \in H_0^1(\Omega). \quad (9.6)$$

473 Then the definition of the  $H^{-1}(\Omega)$  norm together with (9.6) give

$$\|f\|_{H^{-1}(\Omega)} = \sup_{v \in H_0^1(\Omega); \|\nabla v\|_\Omega=1} (f, v) \stackrel{(9.6)}{=} \sup_{v \in H_0^1(\Omega); \|\nabla v\|_\Omega=1} (\nabla\phi, \nabla v) = \|\nabla\phi\|_\Omega.$$

474 We consider the cell-centered finite volume method to find an approximate solution to problem (9.5) on a refined  
 475 mesh. Assuming that the discretization error is negligible, we employ  $\|\nabla\tilde{\phi}_h\|_\Omega$ , where  $\tilde{\phi}_h$  is obtained by a  
 476 postprocessing as in Definition 5.1, to approximate  $\|f\|_{H^{-1}(\Omega)}$ .

477 The results are reported in Table 1 where we show at each smoothing step  $j$  and linearization step  $k$ : the last  
 478 algebraic step  $\bar{i}$ , the estimators, and the effectivity indices (9.4) at convergence of the algebraic solver ( $i = \bar{i}$ ).  
 479 We observe that we indeed have a guaranteed upper bound on all steps  $j \geq 1, k \geq 1$ , and  $\bar{i}$ , and that all the  
 480 effectivity indices take excellent values when all the three stopping criteria (8.1)–(8.3) are satisfied on the last  
 481 line of Table 1.

$j$	$k$	$\bar{i}$	$\eta_{\text{disc}}^{j,k,\bar{i}}$	$\eta_{\text{sm,lin,alg}}^{j,k,\bar{i}}$	$\eta_{\text{lin,alg}}^{j,k,\bar{i}}$	$\eta_{\text{alg}}^{j,k,\bar{i}}$	$\eta^{j,k,\bar{i}}$	$\Gamma_{\text{eff}}^{j,k,\bar{i}}$	$\bar{\Gamma}_{\text{eff}}^{j,k,\bar{i}}$	$\tilde{\Gamma}_{\text{eff}}^{j,k,\bar{i}}$
1	1	12	4.25e-04	8.72e-01	7.06e-01	5.71e-02	8.74e-01	1.70	1.64	2.01
1	2	12	4.27e-04	9.78e-01	1.19e-01	6.83e-04	9.78e-01	1.68	1.63	1.93
1	3	12	4.33e-04	9.97e-01	2.52e-02	4.18e-04	9.97e-01	1.68	1.64	1.93
1	4	12	4.37e-04	1.00e+00	3.85e-03	2.67e-04	1.00e+00	1.69	1.64	1.94
1	5	16	4.37e-04	1.00e+00	1.86e-04	8.24e-08	1.00e+00	1.69	1.64	1.94
1	6	16	4.37e-04	1.00e+00	9.45e-07	1.62e-09	1.00e+00	1.69	1.64	1.94
2	1	20	3.00e-01	7.01e+01	7.05e+01	2.13e+00	7.22e+01	151.79	48.19	77.87
2	2	16	8.30e-02	3.79e+00	7.29e+01	4.13e+00	7.96e+00	65.88	29.01	56.04
2	3	12	1.84e-02	9.17e-01	4.34e+00	3.40e-01	1.20e+00	25.48	11.15	14.50
2	4	12	4.21e-04	3.85e-01	1.50e+00	1.13e-01	4.17e-01	22.16	6.31	11.47
2	5	12	4.18e-04	9.69e-02	2.62e-01	4.39e-03	9.70e-02	4.39	1.97	2.75
2	6	12	4.18e-04	9.90e-02	4.03e-03	1.61e-04	9.90e-02	4.23	1.97	2.67
2	7	12	4.18e-04	9.98e-02	1.79e-03	7.77e-05	9.98e-02	4.14	1.96	2.65
2	8	12	4.18e-04	1.00e-01	6.58e-04	2.69e-05	1.00e-01	4.11	1.96	2.65
2	9	12	4.18e-04	1.00e-01	8.76e-05	5.92e-06	1.00e-01	4.10	1.96	2.64
2	10	12	4.18e-04	1.00e-01	1.45e-06	1.31e-07	1.00e-01	4.10	1.96	2.64
3	1	16	1.26e-02	1.49e+00	1.54e+00	7.12e-02	1.56e+00	41.57	16.06	18.80
3	2	12	5.36e-03	2.64e-01	1.33e+00	9.34e-02	3.53e-01	11.27	4.45	7.08
3	3	28	7.85e-03	3.27e-01	3.40e-01	1.32e-02	3.36e-01	75.10	6.38	11.35
3	4	28	2.68e-03	1.80e-01	3.72e-01	2.68e-02	2.00e-01	80.34	4.32	7.57
3	5	20	1.39e-03	2.94e-02	2.19e-01	2.09e-02	4.28e-02	30.01	1.71	2.60
3	6	48	6.67e-04	9.65e-03	8.62e-03	5.94e-04	9.71e-03	9.46	1.15	1.31
3	7	60	4.08e-04	9.81e-03	5.42e-04	9.94e-06	9.81e-03	11.60	1.16	1.32
3	8	44	4.09e-04	9.94e-03	4.38e-04	4.27e-05	9.95e-03	12.09	1.16	1.32
3	9	48	4.09e-04	9.99e-03	1.13e-04	9.02e-06	1.00e-02	11.67	1.16	1.32
3	10	40	4.09e-04	1.00e-02	2.47e-05	1.35e-06	1.00e-02	11.49	1.16	1.32
⋮	⋮	⋮	⋮	⋮	⋮	⋮	⋮	⋮	⋮	⋮
6	1	24	4.90e-04	3.50e-03	3.50e-03	3.01e-04	4.19e-03	10.26	1.07	1.14
6	2	12	6.13e-04	1.51e-04	3.98e-03	3.66e-04	8.70e-04	2.13	1.01	1.03
6	3	48	4.25e-04	2.02e-03	2.02e-03	1.85e-04	2.60e-03	6.37	1.04	1.09
6	4	16	4.85e-04	8.02e-06	2.34e-03	2.25e-05	4.32e-04	1.06	1.00	1.01
6	5	64	4.07e-04	8.41e-04	8.34e-04	2.61e-05	1.26e-03	3.08	1.01	1.04
6	6	8	4.34e-04	2.44e-05	8.69e-04	7.59e-05	4.79e-04	1.17	1.00	1.01
6	7	248	4.02e-04	3.31e-03	3.30e-03	1.50e-04	3.85e-03	9.42	1.06	1.13
6	8	8	4.19e-04	1.28e-05	3.50e-03	2.00e-05	4.22e-04	1.03	1.00	1.01
6	9	664	4.01e-04	1.00e-05	2.96e-07	2.75e-08	4.01e-04	1.00	1.00	1.01

Table 1: [Adaptive inexact smoothing Newton-min method, Algorithm 1] Last algebraic step  $\bar{i}$ , estimators (7.20) and effectivity indices (9.4) at each smoothing step  $j$  and each Newton-min step  $k$ , at convergence of the algebraic solver ( $i = \bar{i}$ ).

482 We next plot in Figure 10, left, the evolution of the various estimators as a function of the smoothing  
483 iterations in  $j$  when the stopping criteria (8.2) and (8.1) have been satisfied. The curve of the smoothing  
484 estimator goes down at each smoothing step while the discretization estimator stagnates. In the right part,  
485 we show the relative total residual  $\mathbf{R}_{\text{rel}}^{j,k,\bar{i}} := \|\mathbf{R}(\mathbf{X}^{j,k,\bar{i}})\|/\|\mathbf{R}(\mathbf{X}^0)\|$  with  $\mathbf{R}(\cdot)$  given in (9.1) and the relative  
486 linearization residual  $\mathbf{R}_{\text{lin,rel}}^{j,k,\bar{i}} := \|\mathbf{R}_{\text{lin}}(\mathbf{X}^{j,k,\bar{i}})\|/\|\mathbf{R}_{\text{lin}}(\mathbf{X}^{1,0})\|$  with  $\mathbf{R}_{\text{lin}}(\cdot)$  given in (9.2) during the smoothing  
487 iterations. Let us point out that  $\mathbf{R}_{\text{rel}}^{j,k,\bar{i}}$  steadily decreases as we tighten the smoothing. The residual  $\mathbf{R}_{\text{lin,rel}}^{j,k,\bar{i}}$  in  
488 turn systematically takes smaller values. The estimators as a function of the cumulated Newton-min iterations  
489 are then illustrated in Figure 11. We remark that at each smoothing step the linearization estimator and the  
490 algebraic estimator (blue) steadily decrease, while the discretization estimator roughly stagnates. The oscillating  
491 behavior of  $\eta_{\text{sm,lin,alg}}^{j,k,\bar{i}}$  is explained by the fact that it involves  $\eta_{\text{sm,lin,alg},1}^{j,k,\bar{i}}$  given in (7.1d) that takes values varying  
492 between 0 and 6.91e+01 depending on whether the constraint  $\lambda_h^{j,k,\bar{i}} \geq 0$  is satisfied or not. Moreover, Figure 12  
493 shows the evolution of the estimators during the cumulated algebraic steps of the first two smoothing steps. As  
494 expected, the discretization and smoothing estimators typically stagnate while the algebraic estimator decreases  
495 until step  $\bar{i}$ , at which criterion (8.1) is satisfied.

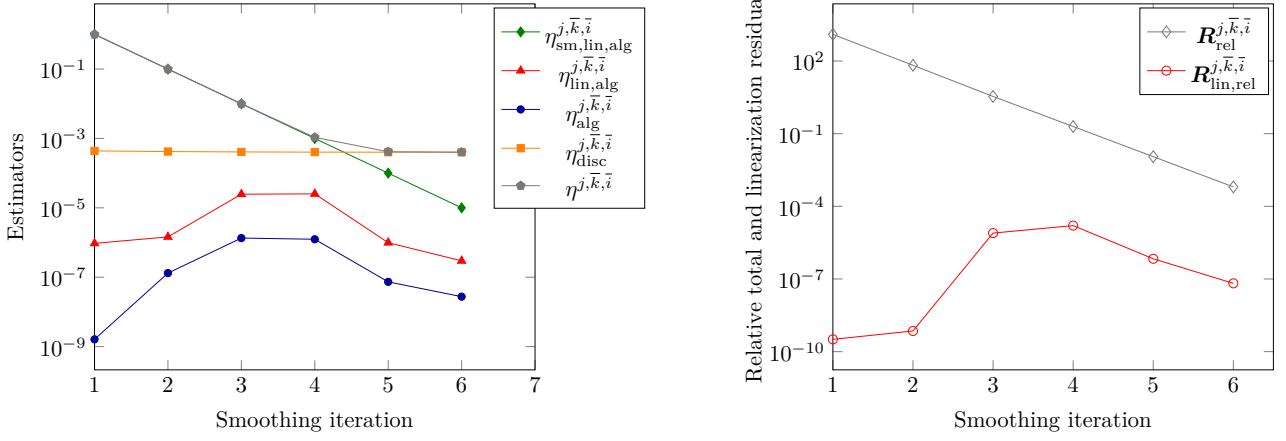


Figure 10: [Adaptive inexact smoothing Newton-min method, Algorithm 1] Estimators of Section 7.3, left, and relative linearization and total residuals, right, as a function of the smoothing iterations  $j$  at convergence of the algebraic and linearization solvers ( $j$  varies,  $k = \bar{k}$ ,  $i = \bar{i}$ ).

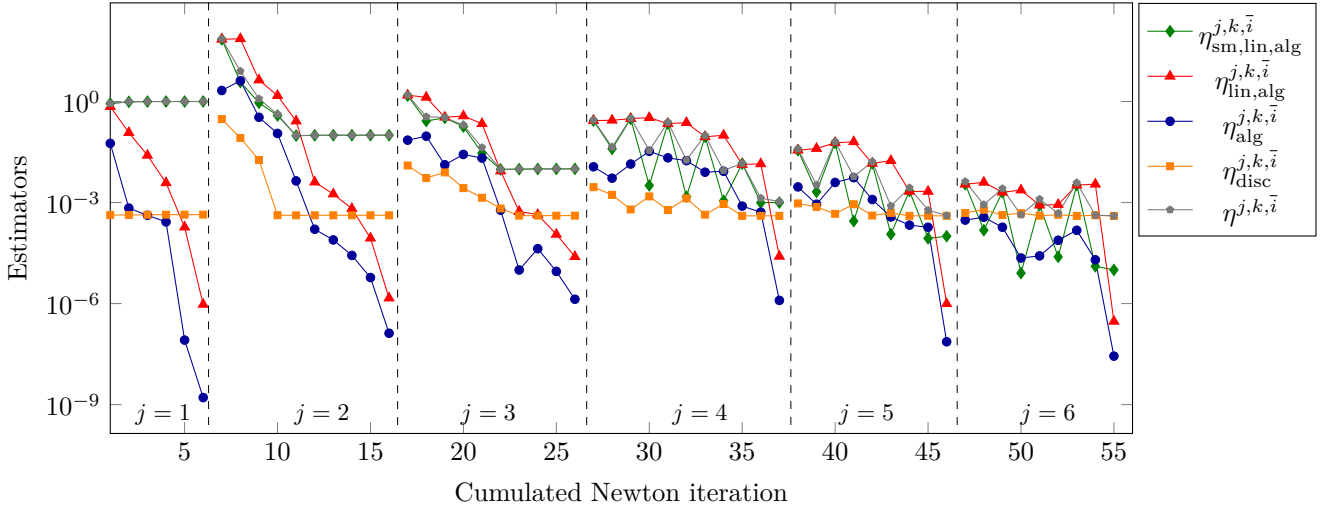


Figure 11: [Adaptive inexact smoothing Newton-min method, Algorithm 1] Estimators of Section 7.3 as a function of the cumulated Newton-min iterations at convergence of the algebraic solver ( $j$  and  $k$  vary,  $i = \bar{i}$ ).

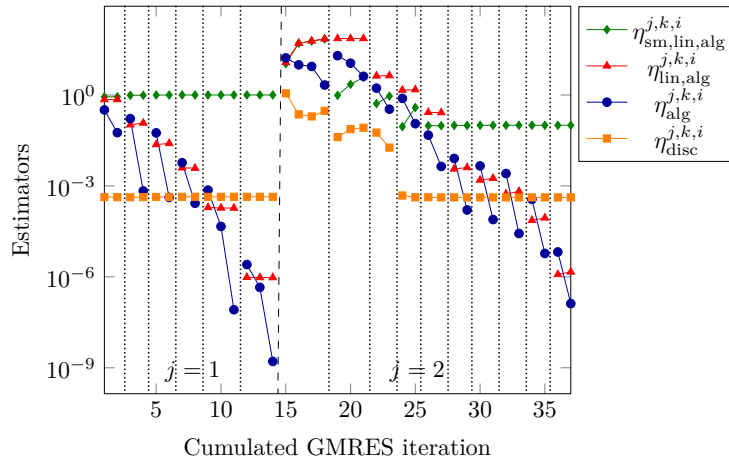


Figure 12: [Adaptive inexact smoothing Newton-min method, Algorithm 1] Estimators of Section 7.3 as a function of the GMRES iterations during the first 2 smoothing iterations ( $j = \{1, 2\}$ ,  $k$  and  $i$  vary).

496 Next, Figure 13 shows the effectivity indices (9.4) during the cumulated Newton-min iterations. It can be  
 497 seen that the index  $\Gamma_{\text{eff}}^{j,k,\bar{i}}$  defined as the ratio of the total error estimator and the actual energy error takes bigger

498 values than the indices  $\tilde{\Gamma}_{\text{eff}}^{j,k,\bar{i}}$  featuring the jump term and the estimate  $\tilde{\Gamma}_{\text{eff}}^{j,k,\bar{i}}$  featuring the jump term and the  
 499 action. When the stopping criteria (8.1)–(8.3) are reached, all the indices approach the optimal value of one.

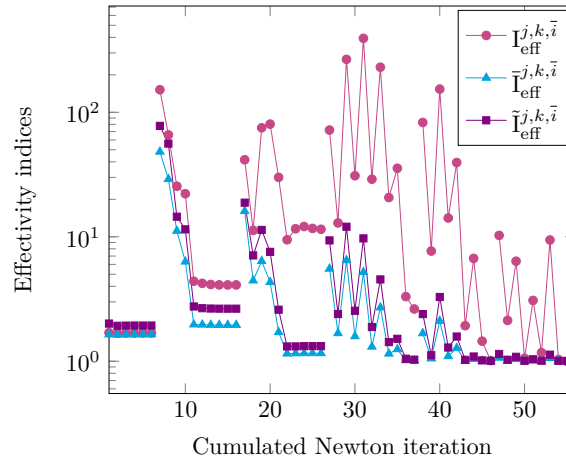


Figure 13: [Adaptive inexact smoothing Newton-min method, Algorithm 1] Effectivity indices given in (9.4) using the total estimator  $\eta^{j,k,\bar{i}}$  given in (7.2), as a function of the cumulated Newton-min iterations, at convergence of the algebraic solver ( $i = \bar{i}$ ).

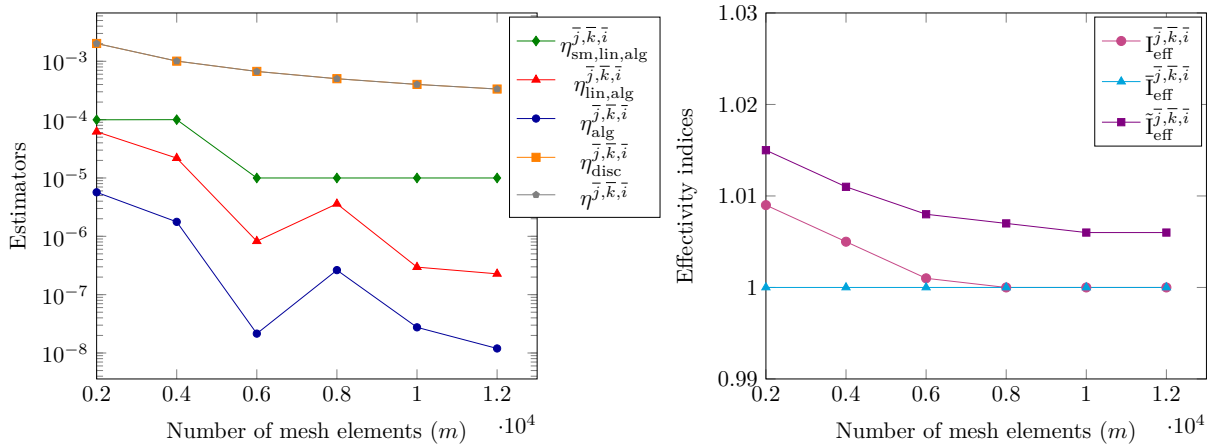


Figure 14: [Adaptive inexact smoothing Newton-min method, Algorithm 1] Estimators, left, and effectivity indices, right, as a function of the number of mesh elements  $m$  at convergence of all the solvers.

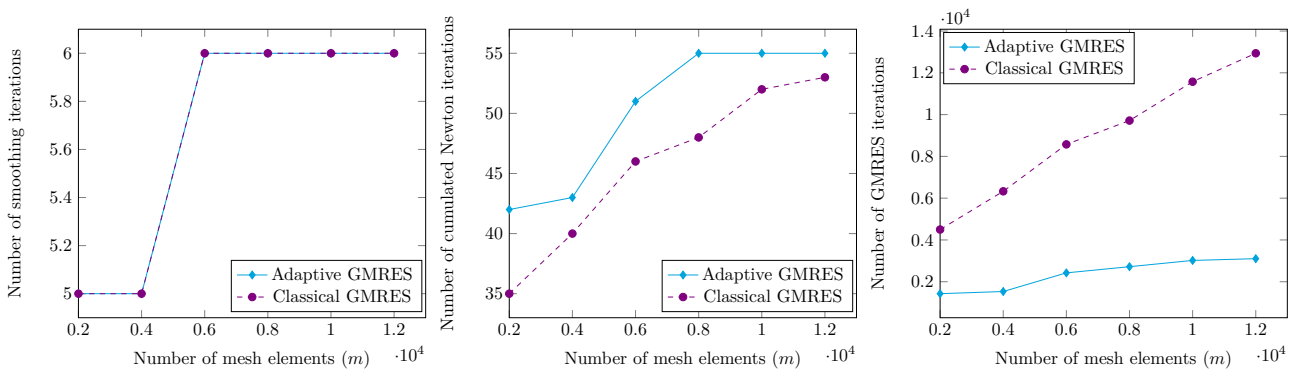


Figure 15: [Adaptive inexact smoothing Newton-min method, Algorithm 1] Number of smoothing iterations (left), cumulated Newton-min iterations (center), and of cumulated algebraic iterations (right) as a function of the number of mesh elements, employing the adaptive stopping criterion (8.1) and the classical one (9.3) for stopping the GMRES solver.

500 The estimators and the effectivity indices at convergence of all solvers, i.e., when the criteria (8.1), (8.2),  
 501 and (8.3) have been satisfied, are plotted in Figure 14 as a function of the number of mesh elements. Notice

502 that the discretization estimator essentially coincides with the total estimator. We observe that the accuracy  
 503 of our estimators increases in function of the computational effort.

504 We are also interested in the comparison between the adaptive GMRES (adaptive stopping criterion (8.1))  
 505 and the classical GMRES (standard stopping criteria (9.3)) with regard to the number of performed iterations.  
 506 As seen from Figure 15, the adaptive algebraic resolution does not impact the number of smoothing steps. It  
 507 slightly affects the number of cumulated Newton steps but leads to an important decrease of the number of  
 508 GMRES iterations compared with the classical resolution. In this regard, we numerically explore the influence  
 509 of the coefficients  $\zeta_{\text{sm}}$ ,  $\zeta_{\text{lin}}$ , and  $\zeta_{\text{alg}}$  in the adaptive stopping criteria of Section 8 on the smoothing algorithm.  
 510 We summarize the results obtained in Table 2. We observe that choosing  $\zeta_{\text{sm}}$  or  $\zeta_{\text{lin}}$  small does not considerably  
 511 affect the overall number of iterations. However, setting  $\zeta_{\text{alg}}$  small increases notably the number of algebraic  
 512 and linearization iterations.

$\zeta_{\text{sm}}$	$\zeta_{\text{lin}}$	$\zeta_{\text{alg}}$	# Smoothing iter.	# Newton iter.	# GMRES iter.	$\mathbf{R}_{\text{rel}}^{\bar{j}, \bar{k}, \bar{i}}$
$10^{-1}$	$10^{-1}$	$10^{-1}$	6	55	3020	6.33e-04
$10^{-2}$	$10^{-2}$	$10^{-2}$	7	81	9564	3.43e-05
$10^{-2}$	$10^{-1}$	$10^{-1}$	8	59	3104	1.15e-04
$10^{-1}$	$10^{-2}$	$10^{-1}$	6	59	3288	6.33e-04
$10^{-1}$	$10^{-1}$	$10^{-2}$	6	74	8172	6.33e-04

Table 2: [Adaptive inexact smoothing Newton-min method, Algorithm 1] Number of smoothing, cumulated  
 Newton, and cumulated GMRES iterations as well as the relative total residual  $\mathbf{R}_{\text{rel}}^{\bar{j}, \bar{k}, \bar{i}}$  for various parameters  
 $\zeta_{\text{sm}}$ ,  $\zeta_{\text{lin}}$ , and  $\zeta_{\text{alg}}$  in the adaptive stopping criteria of Section 8.

## 513 10 Conclusions and outlook

514 The motivation of the present work was to propose an adaptive inexact smoothing Newton method based on  
 515 rigorous a posteriori error estimates for solving nonlinear algebraic systems with complementarity constraints  
 516 arising from finite volume discretizations. We considered in particular the problem modeling the contact between  
 517 two membranes. We treated the non-differentiable nonlinearity in the constraints by means of a smoothed C-  
 518 function, which allowed a direct application of the standard Newton method. We designed a posteriori error  
 519 estimates between the exact and approximate solution, enabling to identify the error components (discretization,  
 520 smoothing, linearization, algebraic) and yielding adaptive stopping criteria. These criteria together with a simple  
 521 way of tightening the smoothing became the cornerstones of the developed adaptive algorithm. We finally  
 522 provided numerical tests employing our adaptive method and the existing semismooth Newton method. The  
 523 results agree with theoretical developments and confirm that the adaptivity allows for important computational  
 524 savings in terms of number of iterations. Future work will consist in applying this method to several synthetic  
 525 cases of petroleum reservoir simulation, see [33].

## 526 A Appendix

527 The a posteriori estimate (7.3) of Section 7.1 involves the  $L_2$ -norm of  $\lambda_h^{j,k,i,\text{neg}}$  and the global domain diameter  
 528  $h_\Omega$ . This gives a guaranteed upper bound, but is not very sharp. We present here an alternative upper bound  
 529 on the energy error that is typically sharper, but not guaranteed anymore.

**Remark A.1** (Alternative bound). *From (7.11a),  $-b(\mathbf{w}, \lambda_h^{j,k,i})$  can be decomposed as follows*

$$\begin{aligned}
 -b(\mathbf{w}, \lambda_h^{j,k,i}) &= -\left(\lambda_h^{j,k,i}, (u_1 - \tilde{s}_{1h}^{j,k,i}) - (u_2 - \tilde{s}_{2h}^{j,k,i})\right) \\
 &\approx \frac{1}{2} \left\{ \sum_{K \in \mathcal{T}_h} 2 \left( \lambda_h^{j,k,i}, u_{2h}^{j,k,i} - u_{1h}^{j,k,i} + \tilde{s}_{1h}^{j,k,i} - \tilde{s}_{2h}^{j,k,i} \right)_K \right\}.
 \end{aligned}$$

530 This will give us the following result

$$\left\| \mathbf{u} - \tilde{\mathbf{u}}_h^{j,k,i} \right\| \lesssim \eta_{\text{alt}}^{j,k,i} := \left\{ \left( \eta_{\text{osc}} + \eta_{\text{alg}}^{j,k,i} + \eta_{\text{nonc}}^{j,k,i} \right)^2 + \sum_{K \in \mathcal{T}_h} 2 \left( \lambda_h^{j,k,i}, u_{2h}^{j,k,i} - u_{1h}^{j,k,i} + \tilde{s}_{1h}^{j,k,i} - \tilde{s}_{2h}^{j,k,i} \right)_K \right\}^{\frac{1}{2}}. \quad (\text{A.1})$$

531 The corresponding effectivity indices are illustrated during the cumulated linearization iterations in Figure  
 532 16. We indeed observe a general improvement at the effectivity indices, though they become (importantly)  
 533 below one at the initial iterations.

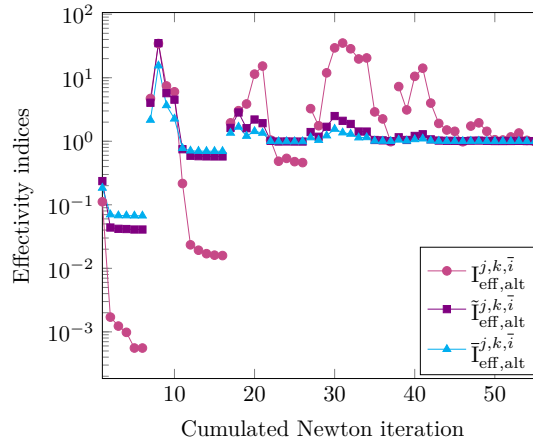


Figure 16: [Adaptive inexact smoothing Newton-min method, Algorithm 1] Effectivity indices using the alternative total estimator  $\eta_{\text{alt}}^{j,k,i}$  as a function of the cumulated Newton-min iterations, at convergence of the algebraic solver ( $i = \bar{i}$ ).

## 534 References

- 535 [1] M. AINSWORTH, *Robust a posteriori error estimation for nonconforming finite element approximation*,  
 536 SIAM J. Numer. Anal., 42 (2005), pp. 2320–2341, <https://doi.org/10.1137/S0036142903425112>.
- 537 [2] M. AINSWORTH AND J. T. ODEN, *A posteriori error estimation in finite element analysis*, Pure and  
 538 Applied Mathematics (New York), Wiley-Interscience [John Wiley & Sons], New York, 2000, <https://doi.org/10.1002/9781118032824>.
- 540 [3] M. BEBENDORF, *A note on the Poincaré inequality for convex domains*, Z. Anal. Anwendungen, 22 (2003),  
 541 pp. 751–756, <https://doi.org/10.4171/ZAA/1170>.
- 542 [4] R. BECKER, D. CAPATINA, AND R. LUCE, *Stopping criteria based on locally reconstructed fluxes*, in  
 543 Numerical mathematics and advanced applications—ENUMATH 2013, vol. 103 of Lect. Notes Comput.  
 544 Sci. Eng., Springer, Cham, 2015, pp. 243–251.
- 545 [5] F. BEN BELGACEM, C. BERNARDI, A. BLOUZA, AND M. VOHRALÍK, *A finite element discretization of*  
 546 *the contact between two membranes*, M2AN Math. Model. Numer. Anal., 43 (2009), pp. 33–52, <https://doi.org/10.1051/m2an/2008041>.
- 548 [6] F. BEN BELGACEM, C. BERNARDI, A. BLOUZA, AND M. VOHRALÍK, *On the unilateral contact between*  
 549 *membranes. Part 1: Finite element discretization and mixed reformulation*, Math. Model. Nat. Phenom.,  
 550 4 (2009), pp. 21–43, <https://doi.org/10.1051/mmnp/20094102>.
- 551 [7] F. BEN BELGACEM, C. BERNARDI, A. BLOUZA, AND M. VOHRALÍK, *On the unilateral contact between*  
 552 *membranes. Part 2: a posteriori analysis and numerical experiments*, IMA J. Numer. Anal., 32 (2012),  
 553 pp. 1147–1172, <https://doi.org/10.1093/imanum/drr003>.
- 554 [8] I. BEN GHARIBIA, J. FERZLY, M. VOHRALÍK, AND S. YOUSEF, *Semismooth and smoothing New-*  
 555 *ton methods for nonlinear systems with complementarity constraints: adaptivity and inexact resolu-*  
 556 *tion*, HAL Preprint 03355116, submitted for publication, (2021), <https://hal.archives-ouvertes.fr/hal-03355116>.

- 558 [9] I. BEN GHARIBIA AND J. C. GILBERT, *Nonconvergence of the plain Newton-min algorithm for linear*  
559 *complementarity problems with a P-matrix*, Math. Prog., 134 (2012), pp. 349–364, [https://doi.org/10.](https://doi.org/10.1007/s10107-010-0439-6)  
560 [1007/s10107-010-0439-6](https://doi.org/10.1007/s10107-010-0439-6).
- 561 [10] I. BEN GHARIBIA AND J. JAFFRÉ, *Gas phase appearance and disappearance as a problem with complemen-*  
562 *tarity constraints*, Math. Comput. Simul., 99 (2014), pp. 28–36, [https://doi.org/10.1016/j.matcom.](https://doi.org/10.1016/j.matcom.2013.04.021)  
563 [2013.04.021](https://doi.org/10.1016/j.matcom.2013.04.021).
- 564 [11] J. F. BONNANS, J. C. GILBERT, C. LEMARÉCHAL, AND C. A. SAGASTIZÁBAL, *Numerical optimization*,  
565 Universitext, Springer-Verlag, Berlin, second ed., 2006, <https://doi.org/10.1007/978-3-540-35447-5>.
- 566 [12] D. BRAESS AND J. SCHÖBERL, *Equilibrated residual error estimator for edge elements*, Math. Comp., 77  
567 (2008), pp. 651–672, <https://doi.org/10.1090/S0025-5718-07-02080-7>.
- 568 [13] H. BREZIS, *Functional analysis, Sobolev spaces and partial differential equations*, Universitext, Springer,  
569 New York, 2011, <https://doi.org/10.1007/978-0-387-70914-7>.
- 570 [14] F. BREZZI AND M. FORTIN, *Mixed and hybrid finite element methods*, vol. 15 of Springer Series in Computa-  
571 tional Mathematics, Springer-Verlag, New York, 1991, <https://doi.org/10.1007/978-1-4612-3172-1>.
- 572 [15] M. BÜRG AND A. SCHRÖDER, *A posteriori error control of hp-finite elements for variational inequalities*  
573 *of the first and second kind*, Comput. Math. Appl., 70 (2015), pp. 2783–2802, [https://doi.org/10.1016/](https://doi.org/10.1016/j.camwa.2015.08.031)  
574 [j.camwa.2015.08.031](https://doi.org/10.1016/j.camwa.2015.08.031).
- 575 [16] F. CHOULY, M. FABRE, P. HILD, J. POUSIN, AND Y. RENARD, *Residual-based a posteriori error estima-*  
576 *tion for contact problems approximated by Nitsche’s method*, IMA J. Numer. Anal., 38 (2018), pp. 921–954,  
577 <https://doi.org/10.1093/imanum/drx024>.
- 578 [17] J. DABAGHI, V. MARTIN, AND M. VOHRALÍK, *Adaptive inexact semismooth Newton methods for the*  
579 *contact problem between two membranes*, J. Sci. Comput., 84, 28 (2020), [https://doi.org/10.1007/](https://doi.org/10.1007/s10915-020-01264-3)  
580 [s10915-020-01264-3](https://doi.org/10.1007/s10915-020-01264-3).
- 581 [18] T. DE LUCA, F. FACCHINEI, AND C. KANZOW, *A semismooth equation approach to the solution of*  
582 *nonlinear complementarity problems*, Math. Programming, 75 (1996), pp. 407–439, [https://doi.org/10.](https://doi.org/10.1007/BF02592192)  
583 [1007/BF02592192](https://doi.org/10.1007/BF02592192).
- 584 [19] P. DESTUYNDER AND B. MÉTIVET, *Explicit error bounds in a conforming finite element method*, Math.  
585 Comp., 68 (1999), pp. 1379–1396, <https://doi.org/10.1090/S0025-5718-99-01093-5>.
- 586 [20] D. A. DI PIETRO, E. FLAURAUD, M. VOHRALÍK, AND S. YOUSEF, *A posteriori error estimates, stopping*  
587 *criteria, and adaptivity for multiphase compositional Darcy flows in porous media*, J. Comput. Phys., 276  
588 (2014), pp. 163–187, <https://doi.org/10.1016/j.jcp.2014.06.061>.
- 589 [21] D. A. DI PIETRO, M. VOHRALÍK, AND S. YOUSEF, *Adaptive regularization, linearization, and discretiza-*  
590 *tion and a posteriori error control for the two-phase Stefan problem*, Math. Comp., 84 (2015), pp. 153–186,  
591 <https://doi.org/10.1090/S0025-5718-2014-02854-8>.
- 592 [22] A. ERN AND M. VOHRALÍK, *Adaptive inexact Newton methods with a posteriori stopping criteria for*  
593 *nonlinear diffusion PDEs*, SIAM J. Sci. Comput., 35 (2013), pp. A1761–A1791, [https://doi.org/10.](https://doi.org/10.1137/120896918)  
594 [1137/120896918](https://doi.org/10.1137/120896918).
- 595 [23] A. ERN AND M. VOHRALÍK, *Polynomial-degree-robust a posteriori estimates in a unified setting for con-*  
596 *forming, nonconforming, discontinuous Galerkin, and mixed discretizations*, SIAM J. Numer. Anal., 53  
597 (2015), pp. 1058–1081, <https://doi.org/10.1137/130950100>.
- 598 [24] R. EYMARD, T. GALLOUËT, AND R. HERBIN, *Finite volume methods*, Handb. Numer. Anal., VII, North-  
599 Holland, Amsterdam, 2000, [https://doi.org/10.1016/S1570-8659\(00\)07005-8](https://doi.org/10.1016/S1570-8659(00)07005-8).
- 600 [25] R. EYMARD, T. GALLOUËT, AND R. HERBIN, *Finite volume approximation of elliptic problems and*  
601 *convergence of an approximate gradient*, Appl. Numer. Math., 37 (2001), pp. 31–53, [https://doi.org/](https://doi.org/10.1016/S0168-9274(00)00024-6)  
602 [10.1016/S0168-9274\(00\)00024-6](https://doi.org/10.1016/S0168-9274(00)00024-6).
- 603 [26] F. FACCHINEI AND C. KANZOW, *A nonsmooth inexact Newton method for the solution of large-scale non-*  
604 *linear complementarity problems*, Math. Program., 76 (1997), pp. 493–512, [https://doi.org/10.1007/](https://doi.org/10.1007/BF02614395)  
605 [BF02614395](https://doi.org/10.1007/BF02614395).

- 606 [27] F. FACCHINEI AND J.-S. PANG, *Finite-dimensional variational inequalities and complementarity problems.*  
607 *Vol. I*, Springer Series in Operations Research, Springer-Verlag, New York, 2003, [https://doi.org/10.](https://doi.org/10.1007/b97544)  
608 [1007/b97544](https://doi.org/10.1007/b97544).
- 609 [28] F. FACCHINEI AND J.-S. PANG, *Finite-dimensional variational inequalities and complementarity problems.*  
610 *Vol. II*, Springer Series in Operations Research, Springer-Verlag, New York, 2003, [https://doi.org/10.](https://doi.org/10.1007/b97543)  
611 [1007/b97543](https://doi.org/10.1007/b97543).
- 612 [29] M. C. FERRIS, O. L. MANGASARIAN, AND J.-S. PANG, eds., *Complementarity: applications, algorithms*  
613 *and extensions*, vol. 50 of Applied Optimization, Kluwer Academic Publishers, Dordrecht, 2001, <https://doi.org/10.1007/978-1-4757-3279-5>.  
614
- 615 [30] M. C. FERRIS AND J. S. PANG, *Engineering and economic applications of complementarity problems*,  
616 *SIAM Rev.*, 39 (1997), pp. 669–713, <https://doi.org/10.1137/S0036144595285963>.
- 617 [31] M. C. FERRIS AND K. SINAPIROMSARAN, *Formulating and solving nonlinear programs as mixed comple-*  
618 *mentarity problems*, vol. 481 of Lecture Notes in Econom. and Math. Systems, Springer, Berlin, 2000,  
619 [https://doi.org/10.1007/978-3-642-57014-8\\_10](https://doi.org/10.1007/978-3-642-57014-8_10).
- 620 [32] Z. GE, Q. NI, AND X. ZHANG, *A smoothing inexact Newton method for variational inequalities with*  
621 *nonlinear constraints*, *J. Inequal. Appl.*, (2017), pp. Paper No. 160, 12. , [https://doi.org/10.1186/](https://doi.org/10.1186/s13660-017-1433-9)  
622 [s13660-017-1433-9](https://doi.org/10.1186/s13660-017-1433-9).
- 623 [33] I. B. GHARBA AND E. FLAURAUD, *Study of compositional multiphase flow formulation using complemen-*  
624 *tarity conditions*, *Oil Gas Sci. Technol. Rev. IFP Energies nouvelles.* , (2019), [https://doi.org/10.2516/](https://doi.org/10.2516/ogst/2019012)  
625 [ogst/2019012](https://doi.org/10.2516/ogst/2019012).
- 626 [34] S. GIANI, L. GRUBIŠIĆ, L. HELTAI, AND O. MULITA, *Smoothed-adaptive perturbed inverse iteration for*  
627 *elliptic eigenvalue problems*, *Comput. Methods Appl. Math.*, 21 (2021), pp. 385–405, [https://doi.org/](https://doi.org/10.1515/cmam-2020-0027)  
628 [10.1515/cmam-2020-0027](https://doi.org/10.1515/cmam-2020-0027).
- 629 [35] J. GONDZIO, *Interior point methods 25 years later*, *European J. Oper. Res.*, 218 (2012), pp. 587–601,  
630 <https://doi.org/10.1016/j.ejor.2011.09.017>.
- 631 [36] C. HAGER AND B. I. WOHLMUTH, *Semismooth Newton methods for variational problems with inequality*  
632 *constraints*, *GAMM-Mitt.*, 33 (2010), pp. 8–24, <https://doi.org/10.1002/gamm.201010002>.
- 633 [37] P. HEID AND T. P. WIHLER, *Adaptive iterative linearization Galerkin methods for nonlinear problems*,  
634 *Math. Comp.*, 89 (2020), pp. 2707–2734, <https://doi.org/10.1090/mcom/3545>.
- 635 [38] M. HINTERMÜLLER, K. ITO, AND K. KUNISCH, *The primal-dual active set strategy as a semis-*  
636 *smooth Newton method*, *SIAM J. Optim.*, 13 (2002), pp. 865–888 (2003), [https://doi.org/10.1137/](https://doi.org/10.1137/S1052623401383558)  
637 [S1052623401383558](https://doi.org/10.1137/S1052623401383558).
- 638 [39] M. HINTERMÜLLER AND K. KUNISCH, *Path-following methods for a class of constrained minimization prob-*  
639 *lems in function space*, *SIAM J. Optim.*, 17 (2006), pp. 159–187, <https://doi.org/10.1137/040611598>.
- 640 [40] K. ITO AND K. KUNISCH, *Lagrange multiplier approach to variational problems and applications*, vol. 15  
641 of Advances in Design and Control, Society for Industrial and Applied Mathematics (SIAM), Philadelphia,  
642 PA, 2008, <https://doi.org/10.1137/1.9780898718614>.
- 643 [41] K. ITO AND K. KUNISCH, *Semi-smooth Newton methods for the Signorini problem*, *Appl. Math.*, 53 (2008),  
644 pp. 455–468, <https://doi.org/10.1007/s10492-008-0036-7>.
- 645 [42] C. KANZOW, *An active set-type Newton method for constrained nonlinear systems*, in *Complementarity:*  
646 *applications, algorithms and extensions* (Madison, WI, 1999), vol. 50 of Appl. Optim., Kluwer Acad. Publ.,  
647 Dordrecht, 2001, pp. 179–200, [https://doi.org/10.1007/978-1-4757-3279-5\\_9](https://doi.org/10.1007/978-1-4757-3279-5_9).
- 648 [43] J. M. MARTÍNEZ AND L. Q. QI, *Inexact Newton methods for solving nonsmooth equations*, *J. Comput.*  
649 *Appl. Math.*, 60 (1995), pp. 127–145, [https://doi.org/10.1016/0377-0427\(94\)00088-I](https://doi.org/10.1016/0377-0427(94)00088-I).
- 650 [44] J. PAPEŽ, U. RÜDE, M. VOHRALÍK, AND B. WOHLMUTH, *Sharp algebraic and total a posteriori error*  
651 *bounds for  $h$  and  $p$  finite elements via a multilevel approach. Recovering mass balance in any situation*,  
652 *Comput. Methods Appl. Mech. Engrg.*, 371 (2020), pp. 113243, 39, [https://doi.org/10.1016/j.cma.](https://doi.org/10.1016/j.cma.2020.113243)  
653 [2020.113243](https://doi.org/10.1016/j.cma.2020.113243).

- 654 [45] M. PICASSO, *A stopping criterion for the conjugate gradient algorithm in the framework of anisotropic*  
655 *adaptive finite elements*, Comm. Numer. Methods Engrg., 25 (2009), pp. 339–355, [https://doi.org/10.](https://doi.org/10.1002/cnm.1120)  
656 [1002/cnm.1120](https://doi.org/10.1002/cnm.1120).
- 657 [46] S. REPIN, *A posteriori estimates for partial differential equations*, vol. 4 of Radon Series on Computational  
658 and Applied Mathematics, Walter de Gruyter GmbH & Co. KG, Berlin, 2008, [https://doi.org/10.1515/](https://doi.org/10.1515/9783110203042)  
659 [9783110203042](https://doi.org/10.1515/9783110203042).
- 660 [47] S. I. REPIN, *Functional a posteriori estimates for elliptic variational inequalities*, J. Math. Sci., 152 (2008),  
661 pp. 702–712, <https://doi.org/10.1007/s10958-008-9093-4>.
- 662 [48] V. REY, C. REY, AND P. GOSSELET, *A strict error bound with separated contributions of the discretization*  
663 *and of the iterative solver in non-overlapping domain decomposition methods*, Comput. Methods Appl.  
664 Mech. Engrg., 270 (2014), pp. 293–303, <https://doi.org/10.1016/j.cma.2013.12.001>.
- 665 [49] S.-P. RUI AND C.-X. XU, *A smoothing inexact Newton method for nonlinear complementarity problems*,  
666 J. Comput. Appl. Math., 233 (2010), pp. 2332–2338, <https://doi.org/10.1016/j.cam.2009.10.018>.
- 667 [50] Y. SAAD AND M. H. SCHULTZ, *GMRES: a generalized minimal residual algorithm for solving nonsym-*  
668 *metric linear systems*, SIAM J. Sci. Statist. Comput., 7 (1986), pp. 856–869, [https://doi.org/10.1137/](https://doi.org/10.1137/0907058)  
669 [0907058](https://doi.org/10.1137/0907058).
- 670 [51] G. STADLER, *Semismooth Newton and augmented Lagrangian methods for a simplified friction problem*,  
671 SIAM J. Optim., 15 (2004), pp. 39–62, <https://doi.org/10.1137/S1052623403420833>.
- 672 [52] G. STADLER, *Path-following and augmented Lagrangian methods for contact problems in linear elasticity*,  
673 J. Comput. Appl. Math., 203 (2007), pp. 533–547, <https://doi.org/10.1016/j.cam.2006.04.017>.
- 674 [53] M. ULBRICH, *Semismooth Newton methods for variational inequalities and constrained optimization prob-*  
675 *lems in function spaces*, vol. 11 of MOS-SIAM Series on Optimization, Society for Industrial and Ap-  
676 plied Mathematics (SIAM), Philadelphia, PA; Mathematical Optimization Society, Philadelphia, PA, 2011,  
677 <https://doi.org/10.1137/1.9781611970692>.
- 678 [54] R. VERFÜRTH, *A posteriori error estimation techniques for finite element methods*, Numerical Mathematics  
679 and Scientific Computation, Oxford University Press, Oxford, 2013, [https://doi.org/10.1093/acprof:](https://doi.org/10.1093/acprof:oso/9780199679423.001.0001)  
680 [oso/9780199679423.001.0001](https://doi.org/10.1093/acprof:oso/9780199679423.001.0001).
- 681 [55] M. VOHRALÍK, *On the discrete Poincaré-Friedrichs inequalities for nonconforming approximations of the*  
682 *Sobolev space  $H^1$* , Numer. Funct. Anal. Optim., 26 (2005), pp. 925–952, [https://doi.org/10.1080/](https://doi.org/10.1080/01630560500444533)  
683 [01630560500444533](https://doi.org/10.1080/01630560500444533).
- 684 [56] M. VOHRALÍK, *Residual flux-based a posteriori error estimates for finite volume and related locally conser-*  
685 *vative methods*, Numer. Math., 111 (2008), pp. 121–158, <https://doi.org/10.1007/s00211-008-0168-4>.
- 686 [57] D. T. S. VU, I. BEN GHARBIA, M. HADDOU, AND Q. H. TRAN, *A new approach for solving nonlinear*  
687 *algebraic systems with complementarity conditions. Application to compositional multiphase equilibrium*  
688 *problems*, Mathematics and Computers in Simulation, 190 (2021), pp. 1243–1274, [https://doi.org/10.](https://doi.org/10.1016/j.matcom.2021.07.015)  
689 [1016/j.matcom.2021.07.015](https://doi.org/10.1016/j.matcom.2021.07.015).
- 690 [58] M. H. WRIGHT, *The interior-point revolution in optimization: history, recent developments, and*  
691 *lasting consequences*, Bull. Amer. Math. Soc., 42 (2005), pp. 39–56, [https://doi.org/10.1090/](https://doi.org/10.1090/S0273-0979-04-01040-7)  
692 [S0273-0979-04-01040-7](https://doi.org/10.1090/S0273-0979-04-01040-7).
- 693 [59] N. XIU AND J. ZHANG, *Some recent advances in projection-type methods for variational inequalities*, in  
694 Proceedings of the International Conference on Recent Advances in Computational Mathematics (ICRACM  
695 2001) (Matsuyama), vol. 152, 2003, pp. 559–585, [https://doi.org/10.1016/S0377-0427\(02\)00730-6](https://doi.org/10.1016/S0377-0427(02)00730-6).
- 696 [60] S. ZHANG, Y. YAN, AND R. RAN, *Path-following and semismooth Newton methods for the variational*  
697 *inequality arising from two membranes problem*, J. Inequal. Appl., 1 (2019), [https://doi.org/10.1186/](https://doi.org/10.1186/s13660-019-1955-4)  
698 [s13660-019-1955-4](https://doi.org/10.1186/s13660-019-1955-4).